Coordination Chemistry Reviews, 84 (1988) 47–83
Elsevier Science Publishers B.V., Amsterdam – Printed in The Netherlands

THE BEHAVIOR OF THE TETRA-μ-PYROPHOSPHITO-DI-PLATINUM(II) ION $Pt_2(P_2O_5H_2)_4^{4-}$ AND RELATED SPECIES

ARDEN P. ZIPP

Chemistry Department, SUNY-Cortland, Cortland, New York 13045 (U.S.A.)

(Received 5 January 1987)

CONTENTS

A. INTRODUCTION

In 1977 the reaction of potassium tetrachloroplatinate with molten phosphorous acid was reported [1] to yield a material which produced an intense green luminescence upon irradiation. This compound was originally thought to be $Pt(OP(OH)_2)_2(P(OH)_3)_2$, which had first been reported in 1961 [2]. In less than ten years, the luminescent species, now known to be the tetra-μ-pyrophosphitodiplatinum(II) ion, $Pt_2(POP)_4^{4-}$, ($POP = P_2O_5H_2^{2-}$), has been shown to exhibit many unusual properties. The purpose of this review is to summarize the results obtained during the last decade and to stimulate further activity during the next.

B. SYNTHESIS

The earliest reports [1,3] of the preparation of the compound responsible for the green luminescence describe the isolation of green or purple solids

from a mixture of K_2PtCl_4 and H_3PO_3 heated to dryness at 110 °C. This compound is now known to be a pale yellow species: the green and purple colors reported earlier have been attributed to partially-oxidized impurities [4]. The yellow product can be obtained free of dark impurities by washing with methanol and acetone and recrystallizing [4] to remove excess phosphorous acid, which appears to catalyze the decomposition of the dimer, or by isolating the species as salts which do not have the same crystal form as the dark impurities [5]. The synthesis has been reported to be improved by evaporating the water under an inert atmosphere, by using barium as the counter-ion, or by starting with Na_2PtCl_4 [6]. Using $Pt(NH_3)_2Cl_2$ in place of K_2PtCl_4 has also been suggested [6] as a means to superior results.

C. STRUCTURE

The dimeric structure of the luminescent species shown in Fig. 1 was established in 1980 by X-ray crystallography and NMR techniques [3]. The

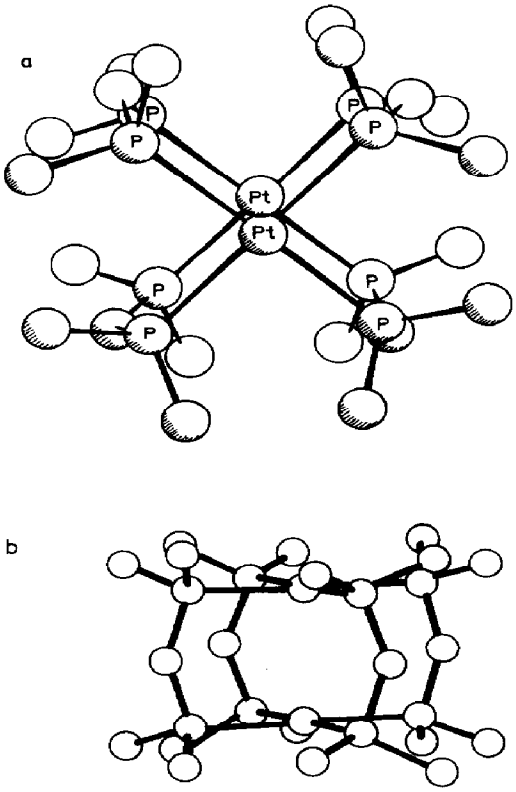

Fig. 1. (a) View of $Pt_2(POP)_4^{4-}$ ion from slightly above Pt–Pt bond. (b) Side view of $Pt_2(POP)_4^{4-}$ ion. (Reprinted with permission from ref. 3.)

compound was placed in the tetragonal space group $P4b2$ with each platinum atom surrounded by a square-planar arrangement of phosphorous atoms in two equivalent pairs, a Pt–Pt separation of 2.925 Å, and approximately four-fold symmetry along the Pt–Pt axis. The X-ray data [7] have been re-analyzed and the coordinates of the bridging units adjusted so that they are equivalent, placing the species in the centrosymmetric space group $P4/mbm$. The Pt–Pt distance within each dimer (2.925 Å) [8] indicates a substantial Pt–Pt interaction, although it has been suggested [9] that the metal–metal distances in bridged species may be more dependent on the bite angles of the bridging ligands than on the intrinsic metal–metal bond strength. The separation between platinum atoms in adjacent units (5.063 Å) suggests little interaction between them. Indeed, the side view of the dimer shown in Fig. 1 indicates that the pyrophosphite units would inhibit the end-on approach of separate units.

The parent compound has been converted to a number of oxidized products, with one or two atoms bonded to the dimeric unit, i.e. $Pt_2(POP)_4X^{4-}$ and $Pt_2(POP)_4XY^{4-}$. The preparation and properties of these compounds will be discussed elsewhere in this review, but their structures will be described here for comparison purposes. In the nine compounds characterized structurally ($Pt_2(POP)_4XY^{4-}$, X = Y = Cl [8,10], Br [11,12], I [11], NO_2 [13,14], SCN [14], imidizaloyl [14], X = CH_3, Y = I [15], $Pt_2(POP)_4X^{4-}$, X = Cl [12] and Br [8]) the added groups occupy axial positions. The Pt–Pt distances, listed in Table 1, are at least 0.1 Å shorter than that in $Pt_2(POP)_4^{4-}$ and are inversely related to the metal oxidation state (vide infra). The similarities of the Pt–P distances (2.35 ± 0.02 Å) and the P–O distances (P=O 1.516 ± 0.009; P–O(H) 1.557 ± 0.016; P–O Br 1.619 ± 0.009 Å) in these compounds suggests that little modification of this portion of the structure occurs upon oxidation. The individual P–O distances (Table 1) are typical of phosphites and pyrophosphates.

The ^{195}Pt NMR spectrum of the compound in D_2O shows a quintet of quintets [3], with each platinum coupled to the four P atoms bonded directly to it and to the four P atoms on the neighboring Pt atom, and it also confirms the presence of the dimer in solution. The Pt chemical shift ($\delta = -5139$ ppm relative to Na_2PtCl_6) and the Pt–P coupling constant ($J = 3075$ Hz) are similar to those found in the monomeric compound $Pt(OP(OMe)_2(HOP(OMe)_2)_2$ ($\delta = -5107$ ppm and $J = 3460$ Hz, respectively) although the P chemical shift in the dimer ($J = 69.4$ ppm) is shifted by 21.5 ppm relative to the methyl ester ($J = 90.9$ ppm). Upon standing, the ^{195}Pt spectrum changes to a simple quintet ($\delta = -5123$ ppm) and the ^{31}P spectrum to a 1:4:1 triplet ($\delta = 86.7$ ppm, $J = 3248$ Hz). These changes have been attributed to the formation of $Pt(OP(OH)_2)_2(P(OH)_3)_2$ during hydrolysis, a compound reported 25 years ago [2].

TABLE 1

Structural data for the $Pt_2(POP)_4^{4-}$ ion and related species

Species	Pt–Pt	Pt–P	P–O(H)	P=O	P–O(br)	Pt–X	Cation		Ref.
$Pt_2(POP)_4^{4-}$	2.925(1)	2.320	1.579	1.519	1.623		$4K^+$	$2H_2O$	3, 7
$Pt_2(PCP)_4^{4-}$	2.980	2.328	1.608	1.530			$4K^+$	$6H_2O$	77
$Pt_2(POP)_4Cl_2^{4-}$	2.695	2.350	1.557	1.512	1.616	2.407	$4K^+$	$2H_2O$	8
$Pt_2(POP)_4Br_2^{4-}$	2.716	2.362	1.556	1.507	1.613	2.572	$4Bu_4N^+$		11
	2.723	2.342	1.529	1.529	1.635	2.555	$4K^+$	$2H_2O$	12
$Pt_2(POP)_4I_2^{4-}$	2.754	2.348	1.565	1.504	1.621	2.746	$4K^+$	$2H_2O$	11
	2.742	2.343	1.535	1.525	1.612	2.721	$2K^+$, $2Bu_4N^+$		11
$Pt_2(POP)_4(SCN)_2^{4-}$	2.760	2.357	1.575	1.500	1.623	2.466	$4K^+$	$2H_2O$	14
$Pt_2(POP)_4(NO_2)_2^{4-}$	2.754	2.372	1.554	1.502	1.633	2.147	$6K^+$ $2NO_2^-$	$2H_2O$	14
$Pt_2(POP)_4(NO_2)_2^{4-}$	2.733	2.380	1.549	1.508	1.632	2.153	$8Na^+$	$18H_2O$	13
		2.3798	1.579	1.496	1.625				
		2.3736	1.561	1.496	1.635				
		2.3779	1.578	1.482	1.611				
$Pt_2(POP)_4CH_3I^{4-}$	2.782	2.339	1.531		1.602	2.18(C) 2.816(I)	$4K^+$	$2H_2O$	15
$Pt_2(POP)_4(imid)_2^{4-}$	2.745	2.362	1.55	1.520	1.628	2.13	$4K^+$	$7H_2O$	14
$Pt_2(POP)_4Cl^{4-}$	2.813	2.329	1.573	1.516	1.621	2.367 2.966	$4K^+$	$2H_2O$	12
$Pt_2(POP)_4Br^{4-}$	2.793	2.334	1.562	1.505	1.618	2.669	$4K^+$	$3H_2O$	12

It is unclear why neither the X-ray nor NMR measurements, which were carried out on green crystals, detected the oxidized impurity. The fact that it is isostructural [10] with the desired material however, suggests that little change would be caused by its inclusion. In addition, very low concentrations may be sufficient to modify the color of the pure yellow crystals.

D. SPECTROSCOPY

The suggestion that the intense luminescence of the $Pt_2(POP)_4^{4-}$ ion is due to a transition within the Pt–Pt bond [3] was made soon after the ion was discovered, but its relation to several unusual aspects of its behavior, including the comparatively long lifetime of its excited state, its very high phosphorescent quantum yield at room temperature, its seemingly anomalous temperature behavior and its delayed fluorescence, have required much more time and effort to determine. In this section an attempt will be made to present a chronology of these discoveries as well as the current state of knowledge about this species.

The intense green luminescence at 514 nm was initially attributed to the excitation of the only absorbance band observed, 368 nm [1]. Additional bands at 285 and 345 nm ($\epsilon = 2800$ and 3000 $M^{-1}\,cm^{-1}$, respectively) were soon reported [3] and the ϵ of the band at 368 nm was calculated to be 30000 $M^{-1}\,cm^{-1}$. Excitation at 368 nm was confirmed to produce the green luminescence, the intensity of which is linear with concentration from 0.2 to 13 μM, but is not observed with hydrolyzed solutions.

A subsequent study [16] yielded a fourth absorbance band ($\lambda = 452$ nm, $\epsilon = 120$ $M^{-1}\,cm^{-1}$) and confirmed the wavelength but revised the extinction coefficient of the band at 368 nm ($\epsilon = 33500$ $M^{-1}\,cm^{-1}$) and reported slight differences for the higher energy bands ($\lambda = 303$ nm, $\epsilon = 849$ $M^{-1}\,cm^{-1}$; $\lambda = 270$ nm, $\epsilon = 1360$ $M^{-1}\,cm^{-1}$). Lowering the temperature of the solid (13–77 K; Nujol) causes slight shifts in the positions of some of the bands ($\lambda = 467$, 399, 299, and 272 nm).

Two emissions were observed in this study rather than one, the intense green band at 515 nm, now attributed to phosphorescence, and a much weaker emission (fluorescence) at 403 nm. The phosphorescence excitation spectrum ($\lambda_{max} = 369$ and 455 nm) overlaps both the fluorescence and phosphorescence bands while the fluorescence excitation spectrum ($\lambda_{max} = 369$ nm) overlaps the emission at 403 nm as shown in Fig. 2. The similarity of the emission behavior of solutions and solids containing the $Pt_2(POP)_4^{4-}$ ion indicates that the dimeric unit is present in both.

The emission and excitation spectra are substantially the same in H_2O at room temperature and in 2 : 1 ethylene glycol–water at 77 K. The phosphorescence spectrum of a solid sample at 75.4 K and the excitation

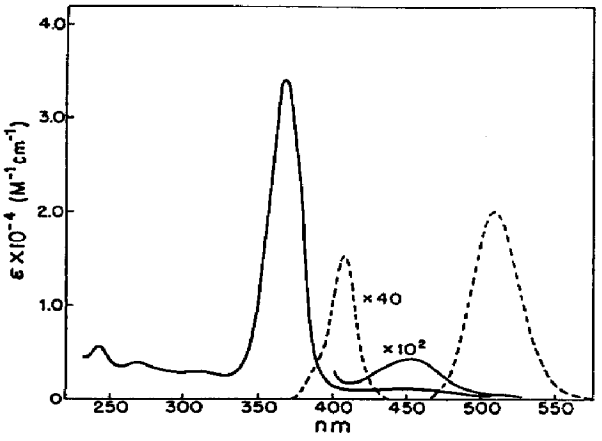

Fig. 2. Absorption (—, ϵ values as given) and corrected emission (— — —) spectra of an aqueous solution of $K_4Pt_2(POP)_4$ (25 °C). (Reprinted with permission from ref. 4.)

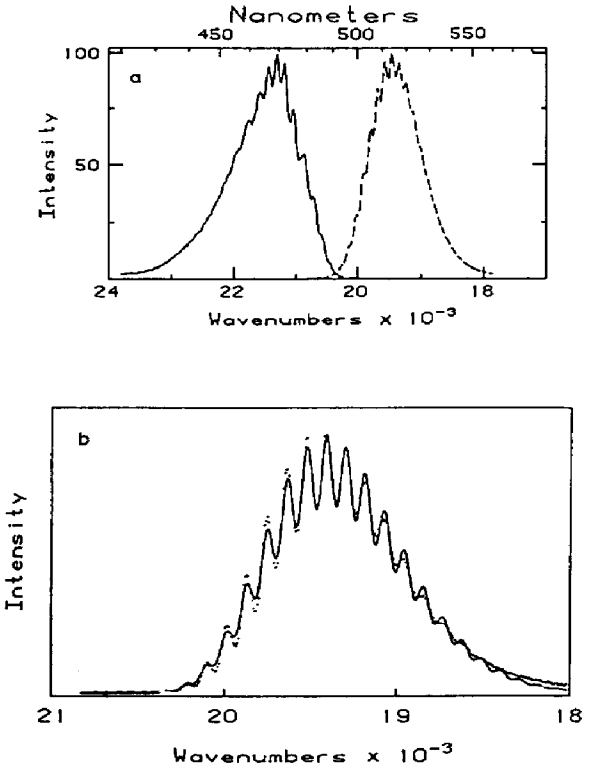

Fig. 3. (a) Phosphorescence excitation (—, 77 K, Nujol mull) and phosphorescence (— — —, 75 K, solid) spectra of $Pt_2(POP)_4^{4-}$. (Reprinted with permission from ref. 16). (b) Phosphorescence spectrum (— — —) of $[Pt_2(POP)_4]^{4-}$ (10.3 K, solid) and computer-generated "best fit" Franck–Condon envelope (———).

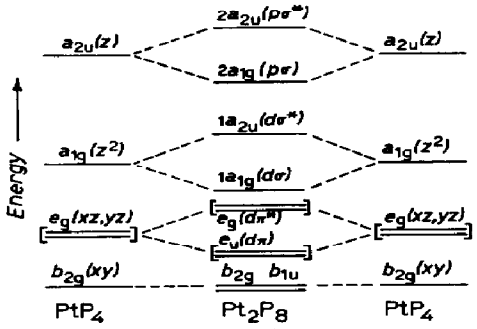

Fig. 4. Simplified MO energy level scheme for $Pt_2(POP)_4^{4-}$. (Reprinted with permission from ref. 24.)

spectrum of a Nujol mull at 77 K overlap at 492 nm (20330 cm^{-1}) and exhibit vibrational fine structure (Fig. 3) with spacings of 139 cm^{-1} (excitation) and 111 cm^{-1} (phosphorescence). A Franck–Condon analysis [17] of the phosphorescence spectrum at 10.3 K shows the apparent origin of the transition to be at 20330 cm^{-1}, in excellent agreement with the energy at which the excitation and phosphorescence spectra overlap. This analysis also yields a value for the Pt–Pt bond vibrational frequency which will be discussed below.

The first attempt [16] to interpret the absorbance and emission data was carried out using the orbital scheme [18] for a Pt(II) ion in D_{4h} symmetry;

$$1a_{1g}(5d_{z^2}) < 1a_{2u}(5d_{z^2}) < 2a_{1g}(6p_z) < 2a_{2u}(6p_z),$$

shown in Fig. 4. With the $1a_{1g}$ and $1a_{2u}$ levels both occupied in the d^8–d^8 $Pt_2(POP)_4^{4-}$ ground state, the absorbance band at 368 nm (27200 cm^{-1}; 25200 cm^{-1} in Nujol) was assigned to $5d_{z^2} \rightarrow 6p_z$, which is the lowest energy-allowed transition; i.e. $^1A_{1g} \rightarrow {}^1A_{2u}$ ($1a_{2u} \rightarrow 2a_{1g}$) and the weak emission at 403 nm (24800 cm^{-1} in H_2O) to the corresponding fluorescence. The weak absorption at 452 nm (22100 cm^{-1}) was assigned to the $^1A_{1g} \rightarrow {}^3A_{2u}$ ($1a_{2u} \rightarrow 2a_{1g}$) transition and the intense emission at 515 nm (19400 cm^{-1}) to the corresponding phosphorescence. Electronic spectra for the $Pt_2(POP)_4^{4-}$ ion and its derivatives are listed in Table 2.

Polarized absorption and emission spectra of single crystals of salts of $Pt_2(POP)_4^{4-}$ at 5 K (Ba^{2+}) and room temperature (K^+) [19] and of the polarization ratios of $K_4Pt_2(POP)_4$ (glycerol–water glass, 160 K) [20] are in accord with these assignments. The strong x, y polarization of the 450-nm band supports its former assignment as $^1A_{1g} \rightarrow {}^3A_{2u}$ and the z polarization of the band at 360 nm suggests that it is due to a $^1A_{1g} \rightarrow {}^1A_{2u}$ transition. Exciting $K_4Pt_2(POP)_4$ at 370 nm with linearly polarized light while monitoring the emission at 400 nm [20] yields a polarization ratio, P, of 0.43,

TABLE 2

Spectroscopic data for $Pt_2(POP)_4^{4-}$ and related species

Species	λ_{abs}	ϵ ($M^{-1}cm^{-1}$)	Assignment [a]	Ref.
Pt(II)–Pt(II)				
$Pt_2(POP)_4^{4-}$	244		A_{2u}	22
	270	1.36×10^3	E_u	16
	303	8.49×10^2	$d \rightarrow d$	
	345	2.80×10^3		
	368	3.45×10^4 (ref. 4)	A_{2u}	
	452	1.2×10^2		
$Pt_2(PCP)_4^{4-}$	382	2.9×10^4		77
	470	1.42×10^2	E_u, A_{1u}	
$Pt_2(POP)_4^{4-}$ *	325			
	470	1.5×10^4		4
$Pt_2(POP)_4^{3-}$	310	7.6×10^4		73
$Pt_2(POP)_4^{5-}$	420	1.3×10^4		47
	600	1.7×10^3		
$Pt_2(POP)_4^{6-}$	373	9.6×10^3		57
	413	1.0×10^4		
	459	1.3×10^4		
Pt(II)–Pt(III)				
$Pt_2(POP)_4Cl^{4-}$	287			39
	355			
	390			
	512 IV (intervalence)			
$Pt_2(POP_4Br^{4-}$	310			39
	355			
	385			
	645 IV			
$Pt_2(POP)_4I^{4-}$	330			39
	370			
	460			
	870 IV			
Pt(III)–Pt(III)				
$Pt_2(POP)_4^{2-}$	245	2.5×10^4		6
	320 br			
$Pt_2(POP)_4^{4-}$	216 [b]	4.9×10^4		10
	282	4.84×10^4		
	345	8.19×10^3		
	385 sh [b]	4.3×10^3		
$Pt_2(POP)_4Br_2^{4-}$	305 (310) (217) [b]	5.54×10^4		10
	345 (358)	1.18×10^4		
	395 sh			
$Pt_2(POP)_4(NO_2)_2^{4-}$	312	2.20×10^4		6
	360 sh	1.21×10^4		
	470 br	6.5×10^2		

TABLE 2 (Continued)

Species	λ_{abs}	ϵ ($M^{-1}cm^{-1}$)	Assignment [a]	Ref.
$Pt_2(POP)_4I_2^{4-}$	338	4.29×10^4		10
	435	1.59×10^4		
$Pt_2(POP)_4(SCN)_2^{4-}$	337	4.36×10^4		6
	367 sh	7.4×10^2		
	480 br			
$Pt_2(POP)_4BrCl^{4-}$	296	3.87×10^4		6
	350	9.5×10^3		
$Pt_2(POP)_4ClI^{4-}$	313	4.1×10^4		38
$Pt_2(POP)_4BrI^{4-}$	316	5.2×10^4		38
$Pt_2(POP)_4$ (imidazolyl)$_2^{4-}$	250			14
$Pt_2(POP)_4CNBr^{4-}$	279			56
	344			
$Pt_2(POP)_4CNI$	294			56
	356			
$Pt_2(POP)_4PhBr^{4-}$	326			51
$Pt_2(POP)_4$ (p-FC_6H_4)Br^{4-}	326			51
$Pt_2(POP)_4PhI^{4-}$	360			51
$Pt_2(POP)_4$ (p-HOC_6H_4)Br^{4-}	321			51
$Pt_2(POP)_4$ (p-$MeOC_6H_4$)Br^{4-}	327			51
$Pt_2(POP)_4PhCl^{4-}$	315			51
$Pt_3(POPOP)_4^{6-}$	580	5.0×10^4		58
$Pt_2(PCP)_4Cl_2^{4-}$	262			77
$Pt_2(PCP)_4Br_2^{4-}$	324			77
$Pt_2(PCP)_4I_2^{4-}$	352			77
	438			

[a] Refs. 10, 22.
[b] Ref. 24.

which is very close to the theoretical value [21] of 0.5 for z excitation followed by z emission and identifies this upper state as A_{2u}, specified further as $^1A_{2u}$ on the basis of the weak transition intensity. Monitoring the emission at 515 nm while exciting at 450 nm produces a value of $P = 0.14$, which suggests $^1A_{1g} \rightarrow E_u(x, y)$ absorption followed by $E_u(x, y) \rightarrow 1A_{1g}$ emission. Further confirmation for this E_u assignment was obtained by monitoring the emission at 515 nm while irradiating the $^1A_{2u}$ band at 400 nm which produced $P = -0.25$ (theory $= -0.33$ for an x, y emission from an E_u state).

A theoretical study [22] verified the assignments of the bands at 368 and 452 nm, assigned the higher energy bands at 36000 cm^{-1} (272 nm) and

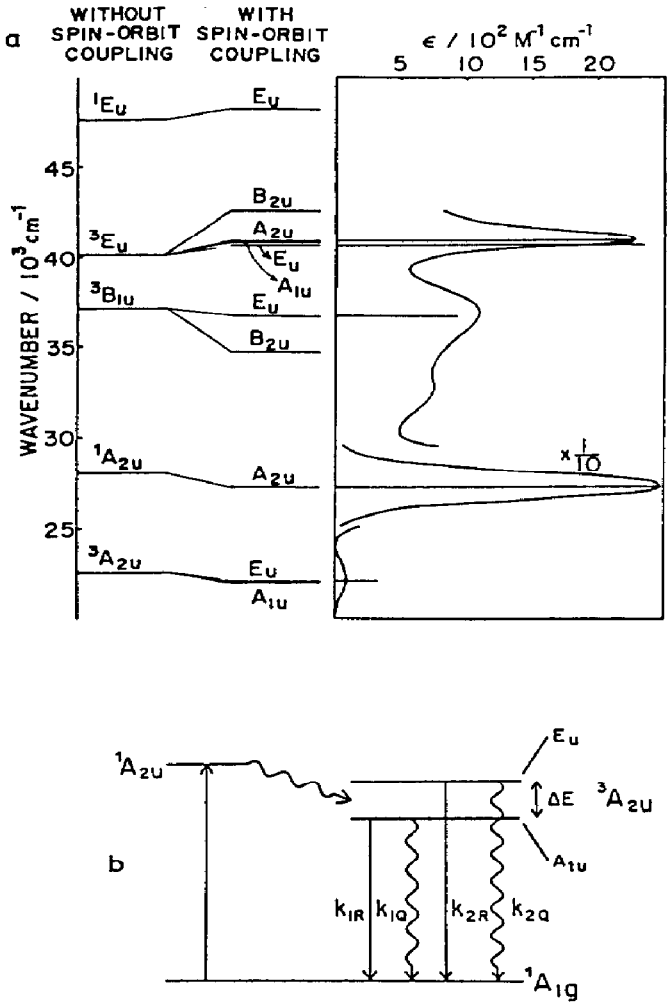

Fig. 5. (a) Calculated and experimental energy level scheme. (Reprinted with permission from ref. 22.) (b) Expanded diagram of pathways relevant to phosphorescent decay. (Reprinted from ref. 27 with permission.)

41000 cm^{-1} (244 nm) to $5d \rightarrow 6p_z$ transitions and attributed the previously unassigned band at 32500 cm^{-1} (303 nm) to a d–d transition. The oscillator strengths calculated agree well with experimental extinction coefficients. The complete energy level scheme from this study is shown in Fig. 5, with and without spin–orbit coupling.

The degenerate (x, y) components of the triplet sublevel (E_u) were determined to lie at a higher energy than the nondegenerate (z component) one (A_{1u}) [22], a finding which was generalized to all binuclear complexes of this electronic type in tetragonal fields, and is observed in certain

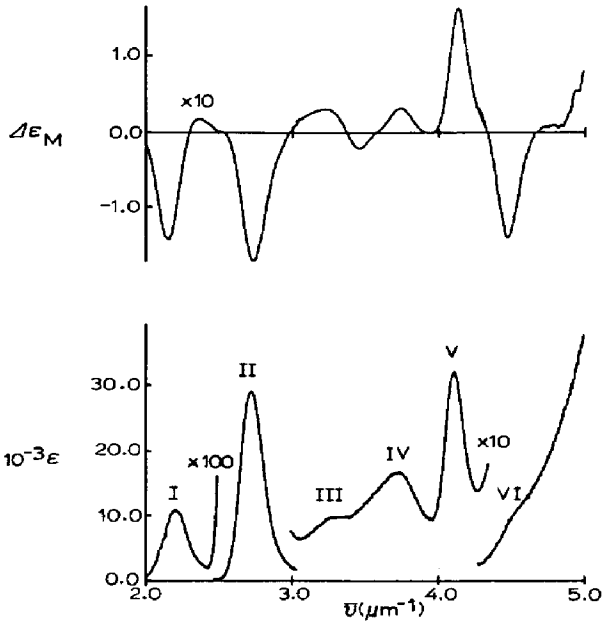

Fig. 6. Electronic absorption (lower curve) and MCD (upper curve) spectra for $K_4[Pt_2(POP)_4]$ in water. (Reprinted from ref. 24 with permission.)

Rh(I)–Rh(I) dimers [23]. It was also concluded that intersystem crossing for $^1A_{2u} \rightarrow {}^3A_{2u}$, for which there is no direct path, takes place through a vibronic spin–orbit perturbation of the Pt–Pt bond, to be discussed later.

The magnetic circular dichroism spectrum shown in Fig. 6 [24] has provided support for several of these assignments. Specifically, the band at 452 nm shows a positive A term (detected from the asymmetry of the strong negative B term) while that at 369 nm exhibits only a negative B term, consistent with transitions to the $E_u(^3A_{2u})$ and $A_{2u}(^1A_{2u})$ states, respectively. The bands at 305 and 270 nm were also assigned to transitions of the $Pt_2(POP)_4^{4-}$ ion, on the basis of differences between their MCD spectra and those of hydrolyzed solutions of the dimer or solutions of the methyl ester, $Pt(P[O][OMe]_2)_2(P[OH][OMe]_2)_2$ [25], despite similarities in absorbance spectra. The MCD features of the band at 305 nm (positive B term at 311 nm and a negative B term at 290 nm) were attributed to transitions to $E_u(^3E_u)$ and $A_{2u}(^3E_u)$. This assignment of the 305 nm band to transitions involving the molecular orbitals of the dimer, i.e., the configuration $(e_u)^3(2a_{1g})$, conflicts with the previous d–d assignment [22], which presumably would occur at the same energy in the monomer and dimer. The band at 270 nm (positive B in MCD) was attributed to $E_u(^3B_{1u})$; $(b_{1u})(2a_{1g})$, in accord with the theoretical assignment [22]. The 245 nm absorbance (strong positive B with a weak A component) was ascribed to $E_u(^1E_u)$; $(e_u)^3$

($2a_{1g}$), in contrast to the theoretical assignment of E_u, A_{1u}, $A_{2u}(^3E_u)$. The MCD of the dichloro and dibromo derivatives were also examined in this study but will be discussed below.

The phosphorescence lifetime [16] first determined as 5.5 μs (deoxygenated H_2O, 298 K) is approximately doubled (10.3 μs) at 77 K in 2 : 1 ethylene glycol–water, a difference which was taken as evidence for a high quantum yield at room temperature, as substantiated more recently by direct measurements. The quantum yield for phosphorescence was found [26] to be 0.52 ± 0.07 in deoxygenated H_2O at 25 °C and 0.43 ± 0.06 (glass, 77 K) but only 0.13 ± 0.06 as a glass at 4.2 K [27]. The value at 77 K is comparable to those for $Ru(bpy)_3^{2+}$ (0.38) and $Ru(phen)_3^{2+}$ (0.60) at that temperature [28].

The lifetime is more than 600 μs at 10 K [16] and was initially reported to decay exponentially between 95 and 9 K but nonexponentially below that. Later, the phosphorescence lifetime for both a green and brown crystalline form of $K_2Pt_2(POP)_4$, as well as that for a 2 : 1 ethylene glycol–water glass [15], were reported to show exponential decays at all temperatures between 1.6 and 300 K. This discrepancy is probably due to differences in experimental conditions since a study [29] in which nonexponential decays were observed at low temperatures found the deviation from exponential behavior to be more pronounced at shorter time intervals and dependent on the intensity of the exciting radiation.

This temperature-dependent behavior has been fitted [15,16] to a dual-emission model in which the two levels (E_u and A_{1u}) are produced from the $^3A_{2u}$ term by spin–orbit coupling as shown in Fig. 5, with emission from the lower level being forbidden and that from the higher level at least partially allowed. The best fits for the non-exponential temperature data [16,29] are obtained for separations of 49.6 cm^{-1} and 45.0 cm^{-1}, respectively, with the lifetime of the lower state (A_{1u}) estimated to be 880 μs and 5.5 ms and that of the upper (E_u) state as 1.58 μs and 2.8 μs. The exponential data [27] yield a smaller value for the E_u–A_{1u} spin–orbit splitting (42 cm^{-1}) and longer lifetimes (6.06 ms, A_{1u}; 4.2 μs, E_u) while a study [19] of the phosphorescence spectrum of $Ba_2Pt_2(POP)_4$ at 5 K gives a value of 40.9 cm^{-1} (vide infra). These values agree reasonably well with one another, especially in view of the diverse conditions under which they were obtained, giving an average ΔE of 44 cm^{-1} and average lifetimes of 4.1 ms (A_{1u}) and 2.9 μs (E_u). The spin–orbit coupling values are very small in comparison with the value for the free Pt(II) ion (4000 cm^{-1}) [30] and even in comparison with the value of 2600 cm^{-1} which has been suggested [31] for use in evaluating molecular properties, although they are comparable to experimental values for Rh(I) monomers (40 cm^{-1}) [32] and somewhat larger than those in Rh(I) dimers (7 cm^{-1}) [33].

Direct evidence for spin–orbit splitting has also been obtained from

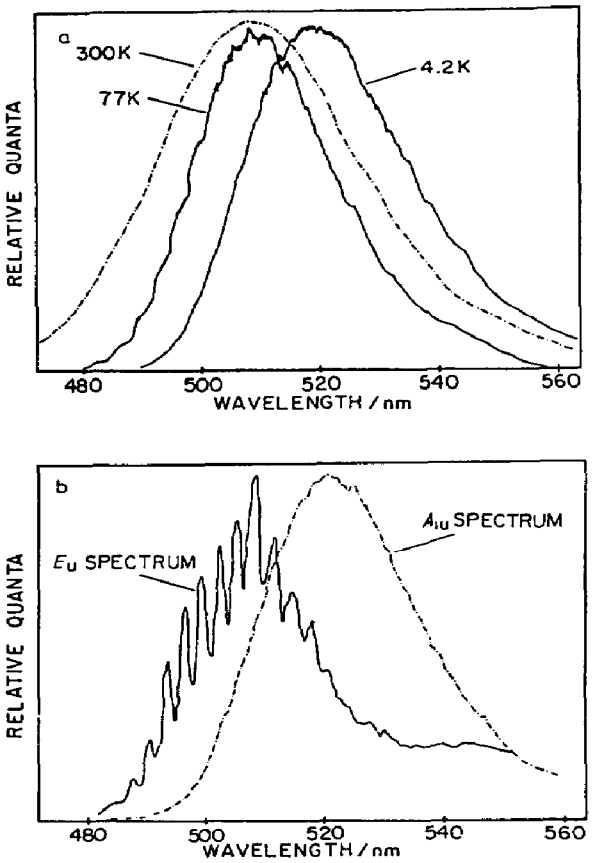

Fig. 7. Phosphorescence spectra of a $K_4Pt_2(POP)_4$ crystal. (a) At different temperatures. (b) At 1.3 K as obtained by time-resolved spectroscopy. (Reprinted from ref. 29 with permission.)

phosphorescence spectra of Ba_2Pt_2 $(POP)_4$ single crystals between 4.2 and 8 K [19]. As the temperature is decreased below 8 K the $^3A_{2u} \rightarrow {}^1A_{1g}$ band at 476. 55 nm decreases in intensity, and a second band appears at 477.48 nm, 40.9 cm^{-1} below the original, clearly suggesting two emitting levels. More recently, calculations [22] have also confirmed that two sublevels exist with an energy separation of 50 cm^{-1} (Fig. 5) and time-resolved phosphorescence spectra [29] have been obtained for the two states (Fig. 7).

The presence of two sublevels has been used to account [29] for the observation (Fig. 7) that the structure which the room temperature emission gains upon cooling to 77 K is gradually lost upon further cooling (and is completely gone at 4.2 K) and for the red shift which the emission maximum (found at 515 nm at temperatures between 300 K and 77 K) exhibits upon further cooling, appearing at ca. 520 nm at 4.2 K. Specifically, only the higher energy $E_u \rightarrow {}^1A_{1g}$ emission is observed at temperatures above 77 K and this emission exhibits an increase in structure with decreasing tempera-

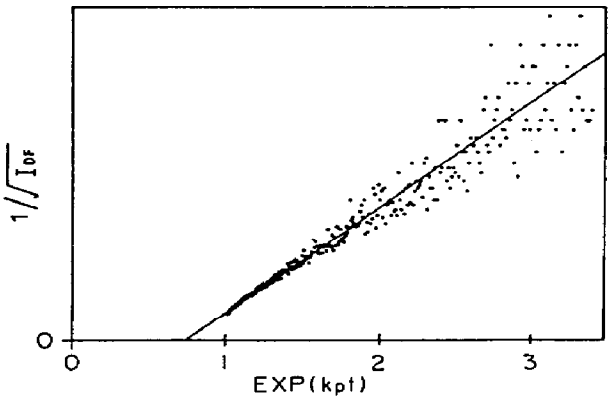

Fig. 8. Plot of the reciprocal of the square root of the delayed fluorescence intensity with respect to $\exp(k_p t)$ where k_p is the first-order phosphorescence decay rate constant. (Reprinted from ref. 34 with permission.)

ture, as expected, whereas only the lower energy (and less structured) $A_{1u} \rightarrow {}^1A_{1g}$ emission is observed at 4.2 K. Thus, the apparent red shift and loss of structure which occurs upon cooling from 77 K to 4.2 K is actually due to a change from one state to another, rather than to the temperature dependence of a single state.

The fluorescence at 407 nm has been found [4] to have a lifetime of less than 2 ns with its intensity unaffected by the addition of O_2. The phosphorescence is quenched significantly, however, both by the addition of O_2 and by the addition of an inner-salt of 1,1′-bis(2-sulfoethyl)-4,4′-bipyridine. The detection of the anion of this salt by flash techniques establishes the quenching mechanism as electron transfer (providing the first evidence for such a process with this species). This behavior will be discussed further in the section on photochemistry below.

Crystals of $K_4Pt_2(POP)_4$ at 4.2 K exhibit anti-Stokes delayed fluorescence ($\lambda_{exc} = 450$ nm, $\lambda_{em} = 395$ nm) with an emission spectrum which is identical to that for normal fluorescence [34]. A plot of the reciprocal of the square root of the intensity of the delayed fluorescence against the exponential $k_p t$ (k_p is the decay rate constant for the triplet state) yields a straight line with a negative intercept, as shown in Fig. 8, the behavior expected for the production of the singlet state ($^1A_{2u}$) by the annihilation of two triplets ($^3A_{2u}$). Although such behavior is fairly common for organic molecules [35], and even for metalloporphyrins [36], it is unusual for an inorganic system.

The high intensity of the emission at 515 nm has prompted its use [37] as a means of detecting low levels of platinum. The intensity–concentration behavior is linear from 10^{-8} to 10^{-6} M at room temperature with a limit of 4 parts per trillion at 77 K and is subject to quenching interference by

Cu(II), Co(II), Pd(II), Rh(III), Ni(II), Fe(II), Ag(I), and Ru(III) but not Cr(III) or Ir(III). The emission intensity is greatest at a pH of 6.5 and is affected only slightly by temperature changes between 0 and 35 °C.

The importance of the Pt–Pt bond to the photophysical (and photochemical) behavior of this species has prompted much interest in the changes which occur in it upon electronic excitation. A Franck–Condon analysis of the phosphorescence spectrum at 10.3 K yields [16] a vibrational frequency of 118 cm^{-1} for the Pt–Pt bond (compared with a value of 116 cm^{-1} obtained in an infrared and Raman study [38]) with an anharmonicity of 0.26 cm^{-1}, and a ratio for the excited-state to ground-state vibrational frequency (k^2) of 0.72. Direct consideration of the vibrational fine structure in the excitation and phosphorescence spectra gives a value of k^2 of 1.25, raising the question of whether the species expands or contracts upon excitation. (The currently accepted view is that it contracts.)

The major vibrational bands assigned from infrared and Raman spectra [38] for Pt(II)–Pt(II) and Pt(III)–Pt(III) species and resonance Raman results [39] for Pt(II)–Pt(III) compounds show little change in the modes due to the $P_2O_5H_2^{2-}$ units upon oxidation of the platinum atoms or substitution of terminal groups. The Pt(II)–Pt(II) stretching frequency is 116 cm^{-1}, while the Pt(III)–Pt(III) frequencies in the terminally-substituted derivatives vary from 110 to 158 cm^{-1} and the Pt(II)–Pt(III) values from 100 to 152 cm^{-1}, depending on the substituent, as shown in Table 3. The Pt–X stretching frequencies in $Pt_2(POP)_4X_2^{4-}$ decrease in the order Cl > Br > I, while ν_{Pt-I} drops even further when the other substituent is a methyl group. The Pt–X frequencies in $Pt_2(POP)_4X^{4-}$ are all lower than those in the corresponding dihalo species due to bridging between two diplatinum units. (A complete listing of overtone and combination bands and their assignments can be found in the original references.)

A normal coordinate analysis [38] of the X–Pt–Pt–X unit in the presence and absence of the pyrophosphite bridging units shows stretching frequencies which agree well with those observed experimentally. The force constant obtained for the platinum–platinum bond, k(Pt–Pt), 1.7 mdyn $Å^{-1}$, is greater than k(Pt–Pt) for the $Pt_2(POP)_4^{2-}$ unit alone, 0.77 mdyn $Å^{-1}$, suggesting that the Pt–Pt bond is strengthened upon oxidation, in accordance with the earlier prediction based on the platinum(II) orbital model [16]. Values for k(Pt–X) (in mdyn $Å^{-1}$) decrease from Cl (1.65) to Br (1.45) to I (1.2).

Electronic spectra of $K_4Pt_2(POP)_4$ at room temperature and of $Ba_2Pt_2(POP)_4$ at 5 K exhibit low frequency progressions assigned to the Pt–Pt stretch for various electronic states of the molecule [19]. The progression for the Ba^{2+} salt ($\nu_{0\rightarrow 1} = 155$ cm^{-1}) has been assigned to the Pt–Pt stretch in the $^3A_{2u}$ excited state and a very low frequency progression (40

TABLE 3

Vibrational frequencies for Pt–Pt and Pt–X bonds

Species	ν_{Pt-Pt} (cm^{-1})	ν_{Pt-X} (cm^{-1})	Ref.
$Pt_2(POP)_4^{4-}$	116		38
	155 (Pt–Pt*)		19
$Pt_2(POP)_4Cl_2^{4-}$	158	295 (IR)	8, 38
		304 (R)	
$Pt_2(POP)_4Br_2^{4-}$	134	195 (IR)	
		224 (R)	
$Pt(POP)_4I_2^{4-}$	110	118 (IR)	
		195 (R)	
$Pt_2(POP)_4CH_3I^{4-}$	156	115 (IR)	
		172 (R)	
		489 (Pt–C)	
$Pt_2(POP)_4(NO_2)_2^{4-}$	151	267	13
$Pt_2(POP)_4(SO_2)_2^{4-}$	111		57
$Pt_2(POP)_4Cl^{4-}$	152	291	39
$Pt_2(POP)_4Br^{4-}$	117	210	39
	122		
$Pt_2(POP)_4I^{4-}$	100	185	39
$Pt_3(POPOP)_4^{6-}$	85 (R)		58
	147 (IR)		

cm^{-1}) to a ligand deformation. The spectra of both salts show a structured band at 400 nm with a progression of 120 cm^{-1}, believed to be due to the Pt–Pt stretch in the electronic ground state. This change in vibrational frequency from 120 to 155 cm^{-1} from the ground to excited state is additional proof for the view that the Pt–Pt bond becomes stronger when an electron is promoted. A Franck–Condon analysis carried out on these structured bands [40] yields an average displacement (assumed to be a contraction) of 0.21 Å.

Time-resolved resonance Raman spectra [41] of aqueous solutions of $Pt_2(POP)_4^{4-}$, obtained by irradiating at 354.7 nm to produce the $^3A_{2u}$ excited state (verified by emission at 410 nm and 520 nm) show a transient absorbance centered at 320 nm. Whereas the ground state spectrum has an intense peak at 118 cm^{-1} (Pt–Pt stretch) with overtones for 2ν and 3ν, the excited spectrum exhibits a new band at 156 cm^{-1} with one overtone. (The overtones exhibit an anharmonicity of ca. 1 cm^{-1} per progression member.) The new band, which increases with the laser pulse energy, is assigned to the excited-state ($3d_{\sigma^*}p_{\sigma}$) Pt–Pt stretch. A shoulder on the 118 cm^{-1} band (102 cm^{-1}) is assigned to a low-energy mode of $^3A_{2u}$, due to its intensity behavior with laser pulse energy.

TABLE 4

Structural and spectroscopic parameters for rhodium(I) dimers

Species	Rh–Rh distance (Å)	ν_{M-M} (cm^{-1})	k(M–M) (mdyn A^{-1})
$Rh_2b_4^{2+}$	3.242 [a]	79 [b]	0.19 [c]
$Rh_2b_4^{2+*}$	2.94 [d]	144 [b]	0.63 [c]
$Rh_2b_4Cl_2^{2+}$	2.837 [e]	134 [c]	0.95 [c]
$Rh(CNPh)_4]_2^{2+}$	3.193 [f]	60 [b]	0.11 [c]
$Rh(CNPh)_4]_2^{2+*}$ (b = 1,3-diisocyanopropane)		162 [b]	0.80 [c]

[a] K.R. Mann, J.A. Thich, R.A. Bell, C.L. Coyle, and H.B. Gray, Inorg. Chem., 19 (1980) 2462.
[b] R.F. Dallinger, V.M. Miskowski, H.B. Gray, and W.H. Woodruff, J. Amer. Chem. Soc., 103 (1981) 1595.
[c] Ref. 41.
[d] Ref. 42.
[e] K.R. Mann, R.A. Bell, and H.B. Gray, Inorg. Chem., 18 (1979) 2761.
[f] K.R. Mann, N.S. Lewis, R.M. Williams, H.B. Gray, and H.J.G. Gordon, Inorg. Chem., 17 (1978) 828.

It is notable that the Pt–Pt bond in both the ground and excited states of $Pt_2(POP)_4^{4-}$ is stronger than the Rh–Rh bond in comparable d^8–d^8 species such as $Rh_2b_4^{2+}$ (b = 1,3-diisocyanopropane) [42] regardless of the criteria used for comparison as shown in Table 4. This behavior is contrary to expectations since rhodium is a 4*d* element and platinum is in the 5*d* series, but has been attributed to constraints imposed by the bridging pyrophosphite ligands [41].

E. PHOTOCHEMISTRY

The phosphorescence of the $Pt_2(POP)_4^{4-}$ ion has been reported to be quenched by both energy and electron transfer pathways. Electron transfer quenching was first reported for the oxidation of the $Pt_2(POP)_4^{4-}$ excited state by the 1,1′-bis(2-sulfoethyl)-4,4′-bipyridinium inner salt (BESP) [4], ($k_q = 5.5 \times 10^9$ M^{-1} s^{-1}). The $BSEP^-$ ion formed (identified by its transient absorption at 610 nm) reacts with the oxidized platinum dimer ($k_q = 1 \times 10^9$ M^{-1} s^{-1}), at a rate near the diffusion-controlled limit. The excited state species also reacts with $Os(NH_3)_5Cl^{2+}$ ($E_{1/2} = -1.09$ V vs. SCE) [43] and nicotinamide ($E_{1/2} = -1.44$ V vs. Ag/AgCl, CH_3OH) [44], demonstrating that it is a stronger reducing agent ($E(3-/4-*) < -1$ V vs. NHE) than $Ru(bpy)_3^{2+}$ ($E = -0.88$ V vs. NHE) [45].

When solutions of the $Pt_2(POP)_4^{4-}$ ion in CH_3CN were subjected to a 4 V AC (280 Hz) potential [46] the green phosphorescence (but not the higher

energy fluorescence) was observed. This behavior was attributed to the conversion of the 4 − ion to a 5 − species at the cathode and a 3 − ion at the anode, with these oxidized and reduced moieties reacting to regenerate two 4 − ions, one of which is in the $^3A_{2u}$ state ($E = 2.6$ V). The absence of fluorescence indicates that the reaction of the 3 − and 5 − ions is not sufficiently energetic to produce the higher energy $^1A_{2u}$ ($E = 3.3$ V) and a short life-time for at least one of the species was inferred from the frequency required. (Pulse radiolysis experiments [47] have shown that the 5 − ion decays in aqueous solution with $k = 2.9 \times 10^4$, see below.) Reductive quenching was not observed, leading to an estimated ground-state reduction potential for the $Pt_2(POP)_4^{4-}$ ion of at least −2.3 V vs. SCE while its oxidation occurs at $E < 1.6$ V vs. NHE [4].

Reductive quenching of the $Pt_2(POP)_4^{4-}$ excited state was observed with a range of electron donors ($0.11 < E < 0.92$V) in methanol [26] for which $k_q = 1.2 \times 10^{10}$ to 1.5×10^6 M^{-1} s^{-1} and $E = 1.1 \pm 0.2$ V for the 4 − */5 − potential, which is greater than that for the $Ru(bpy)_3^{2+}$* reduction, 0.80 V [48]. The smaller k_q values obtained for the reaction of some of the quenchers with the di-platinum excited state (relative to $Ru(bpy)_3^{2+}$*) were ascribed to a greater inner-sphere reorganization energy in the former ($\lambda = 1.4 \pm 0.2$ V vs. 0.5 V), since the outer-sphere requirements were calculated to differ by less than 0.1 V. The $Pt_2(POP)_4^{4-*/5-}$ self-exchange rate was estimated to be $\leqslant 2 \times 10^3$ M^{-1} s^{-1}.

The $Pt_2(POP)_4^{4-}$ emission is affected only slightly by solvent variations [49] (Table 5), although irreproducible quenching was often observed in CH_3CN (offering a possible explanation for the inability of previous workers [46] to observe reductive quenching in that solvent). Phosphorescence quenching rates approach the diffusion-controlled limit for energy acceptor species with triplet levels lower than 2.10 eV, but drop off rapidly for quenchers with E_T greater than this value, consistent with a triplet energy for $Pt_2(POP)_4^{4-}$ suggested by its 515 nm (2.41 eV) emission. In detailed studies with naphthalene ($E_T = 2.63$ eV) and $Ru(bpy)_3^{2+}$ ($E_T = 2.10$ eV), increases in the absorptions due to their triplet states matched the decay of that for the diplatinum triplet, in accordance with direct energy transfer. The efficiency of this energy-transfer process is still in question however, due to the uncertainty about the value of ϵ for triplet $Pt_2(POP)_4^{4-}$. (For example, an energy transfer coefficient of 0.3 was obtained for $\epsilon = 5500 \pm 500$ M^{-1} cm^{-1} at 465 nm, estimated from laser saturation experiments, while an energy-transfer efficiency of 1 requires an ϵ value of 15000 M^{-1} cm^{-1}.)

The rates obtained for reductive quenching reactions represented by the equation

$$Pt_2(POP)_4^{4-*} + Red \rightarrow Pt_2(POP)_4^{5-} + Red^+$$

TABLE 5

Emission behavior of $Pt_2(POP)_4^{4-}$ and related species

Solvent	λ_{exc} (fl)	λ_{em} (fl)	τ	T (K)	λ_{exc} (ph)	λ_{em} (ph)	τ_{deox} (μs)	τ_{aer} (μs)	T (K)	Ref.
$Pt_2(POP)_4^{4-}$										
H_2O	368	403	2 ns	298	368, 452	517	9.5	1.25	298	4, 16
							600		10	16
D_2O		400		298		512	10.0	1.44		49
CH_3OH		400		298		511	9.4	0.38		49
DMF		399		298		511	9.4	0.38		49
CH_3CN		398		298		511	?			49
$Pt_2(PCP)_4^{4-}$										
Nujol						510			77	77
H_2O							0.055		298	
$Pt_3(POPOP)_4^{6-}$										
1 M HCl	580	650	0.5 μs							58

from Stern–Volmer analyses are well below the diffusion controlled limit as had been observed (and attributed to large reorganization requirements) previously [26]. The transient absorbances due to $Pt_2(POP)_4^{4-*}$ ($\lambda = 470$ nm, $\epsilon = 15000\ M^{-1}\ cm^{-1}$) and oxidized products (e.g. DMA^+, $\epsilon_{470} = 2900\ M^{-1}\ cm^{-1}$) were used to obtain cage escape values, estimated to be at least 0.8 ± 0.1 in this case and greater than 0.5 in other instances. The behavior of the DMA^+ transient indicates that the back electron transfer is not quantitative, presumably because the $Pt_2(POP)_4^{5-}$ species decays by other paths as has been suggested by other studies [4,26].

Although oxidative quenching processes give k_q values near the diffusion limit, product yields are very low (e.g. for MV^{2+} yield $< 2\%$) This was ascribed to the formation of ion pairs between the platinum dimer and the positively-charged oxidants, as indicated by the appearance of new absorptions at wavelengths above 400 nm, reported earlier for the interaction of these same oxidants with a number of other species [50]. No evidence for ion-pairing was detected for neutral oxidants such as *N,N'*-diisopropylviologensulfonate (PVS), which reacted according to the equation

$$Pt_2(POP)_4^{4-*} + PVS \rightarrow Pt_2(POP)_4^{3-} + PVS^-$$

Cage escape for this reaction was estimated to be close to unity and k for the back reaction was calculated to be $1.6 \times 10^9\ M^{-1}\ s^{-1}$, in good agreement with the value obtained previously [4].

The excited state species initiates the addition of aryl bromides and iodides to $Pt_2(POP)_4^{4-}$ and the catalytic conversion of isopropyl alcohol to acetone and dihydrogen [51]. Although CH_3I (and other alkyl iodides) add to $Pt_2(POP)_4^{4-}$ thermally [4], aryl compounds ($Ar = C_6H_5$, $X = Br$, I; $Ar =$ *p*-FC_6H_4, *p*-HOC_6H_4, *p*-$MeOC_6H_4$, $X = Br$) do so only upon irradiation [51]. This reaction is halted by adding hydroquinone, SO_2, or acrylonitrile (which quench the phosphorescence at 514 nm), excess bromide ion (in which case $Pt_2(POP)_4Br_2^{4-}$ is the only product observed), or by adding isopropyl alcohol (which leads to the formation of acetone and dihydrogen [51]). The excited state also catalyzes the degradation of chlorocarbons and the hydrogenation of cyclohexene [52] (none of which proceed with the dimer in its ground state), and plays a role in photoinduced substitution reactions between substituted platinum compounds and excess halide ions, including Cl^-, even though aryl chlorides do not add directly (see section on reactivity).

A transient absorption study [53] of the reaction of $Pt_2(POP)_4^{4-}$ with C_6H_5Br, C_6F_5Br, and 1,2-$C_2H_4Br_2$ showed that the last two yield only the dibromo compound, even though all three form $Pt_2(POP)_4Br^{4-}$ initially. (This species undergoes disproportionation to give $Pt_2(POP)_4^{4-}$ and $Pt_2(POP)_4Br_2^{4-}$ with a second-order rate constant of $9.5 \times 10^8\ M^{-1}\ s^{-1}$.)

The evidence in this study also led to a change in the mechanism proposed, from an $S_{RN}1$ pathway (a stepwise electron transfer process [54]), to one in which a bromine atom is abstracted by the platinum diradical triplet excited state, as had been suggested previously [51] for the formation of dihydrogen and acetone from isopropyl alcohol (vide infra). Regardless of the mechanism involved, this reaction of a Pt(II) species with an aryl compound is quite unusual, since aryl halides usually prefer to add to electron-rich centers such as Pt(0) [55].

TABLE 6

Quenching behavior of $Pt_2(POP)_4^{4-}$ and related species

Quencher	Solvent	$k_q\tau$ (M^{-1} s^{-1})	k_qI (M^{-1} s^{-1})		Ref.
		Energy transfer		E^*	
Oxygen	H_2O	2.4×10^9			49
	CH_3OH	1.4×10^9			49
	DMF	1.5×10^9			49
Azulene	CH_3OH	3.5×10^9	2.6×10^9	1.34 eV	49
Anthracene	CH_3OH		6.2×10^9	1.85 eV	49
$Ru(bpy)_3^{2+}$	H_2O	1.8×10^{10}	4.0×10^{10}	2.10 eV	49
Naphthalene	CH_3OH			2.63 eV	49
Biphenyl	CH_3OH	10^6		2.85 eV	49
		Reductive		$E(D^+/D)$	
1,1′-bis(2-sulfoethyl)-4,4′-bipyridinium	H_2O	5.5×10^9			4
N,N,N′N′-Me_4-1,4-benzenediamine	CH_3OH	1.2×10^{10}		0.11 [a]	26
N,N,N′N′-Me_4-(1,1′biphenyl)-4,4′-diamine	CH_3OH	3.0×10^9		0.36	26
N,N′-4-trimethylbenzamine	CH_3OH	3.9×10^7		0.71	26
N,N-dimethylbenzeneamine	CH_3OH	1.2×10^7		0.78	26
N,N-diphenylbenzeneamine	CH_3OH	1.5×10^6		0.92	26
10-methylphenothiazine	CH_3OH	8.0×10^7	6.5×10^7	0.73	49
N,N-diphenylamine	CH_3OH		10^6	0.93	49
N,N,N-triethylamine	CH_3OH		10^6	0.98	49
		Oxidative		$E(A/A^-)$	
N,N-diisopropylviologen-sulfonate	H_2O	4.5×10^9	5.5×10^9	−0.34	49
Methylviologen	H_2O	1.7×10^{10}	4.6×10^{10}	−0.44	49
Cobaltoceniumdicarboxylate	H_2O	1.5×10^9	3.0×10^9	−0.63	49
$Rh(bpy)_3^{3+}$	H_2O	1.5×10^{10}	4.0×10^{10}	−0.72	49
$S_2O_8^{2-}$	H_2O	1.5×10^6			49
CCl_4	CH_3CN		2×10^9		52
$CHCl_3$	CH_3CN		6×10^7		52

[a] $E_{1/2}$ vs. SCE CH_3CN R_4NClO_4.

Adding 2-propanol to solutions of $Pt_2(POP)_4^{4-}$ and aryl halides halts the production of $Pt_2(POP)_4ArX^{4-}$ and leads to acetone and dihydrogen as alternate products [51], which are formed even in the absence of the aryl halide but not when the light is turned off. The reaction is proposed to occur via the initial abstraction of the methine hydrogen from 2-propanol by the $Pt_2(POP)_4^{4-}$ excited state to form $(CH_3)_2\dot{C}OH$ and a hydrido species, followed by the reaction of the hydrido species with a second molecule of alcohol to give a dihydride, or, the reaction of $(CH_3)_2\dot{C}OH$ with a second $Pt_2(POP)_4^{4-}$ ion to yield more of the hydrido species and acetone. Elimination of dihydrogen from the dihydride completes the catalytic cycle which proceeds with a complex turnover number of 400 at a rate of 1.75 M^{-1} in 3h. Dihydrogen is also evolved from cyclohexanol and (in small amounts) from ethanol and methanol.

The photolysis of solutions of $Pt_2(POP)_4^{4-}$ in 2-propanol containing cyclohexene or cyclopentene leads to the production of the saturated species [52] with a turnover number of 370 molecules in 12 h. The turnover number is decreased significantly (~ 50) when 2-propanol is replaced with methanol and no photoreaction is observed with either 1- or 2-hexene.

The direct reaction of the $Pt_2(POP)_4^{4-*}$ excited state with halocarbons has now been extended to CCl_4 and $CHCl_3$ which quench its phosphorescence (but not its fluorescence) with rate constants of 2×10^9 and 6×10^7 M^{-1} s^{-1}, respectively [52]. The process is thought to involve the formation of a chlorocarbon radical anion and $Pt_2(POP)_4^{3-}$, which then react to give $Pt_2(POP)_4Cl^{4-}$ and the alkyl radical. In de-aerated solutions, these species interact to give the addition compound $Pt_2(POP)_4(R)(Cl)^{4-}$ as shown by a decrease in absorbance at 368 nm and an increase at 337 nm (λ_{max} for ArCl addition species occurs at 310 nm [51]). The final product in the presence of O_2, which scavenges alkyl radicals, is the dichloro species ($\lambda_{max} = 282$ nm), formed by disproportionation as reported previously [8]. Dichloromethane, with a more negative E^0 than $CHCl_3$ or CCl_4, does not react.

A summary of all quenching results obtained to date is given in Table 6.

F. REACTIVITY

Although interest in the $Pt_2(POP)_4^{4-}$ ion developed initially because of its intense luminescence and the chemistry of its excited state, a substantial chemistry of its ground state has also emerged. Hydrolysis [6,37], oxidative addition [6,8,10,14,39,56], addition without oxidation [27,57] and reduction [27] reactions have all been reported and all lead to a loss of luminescence. A higher oligomer has been prepared (but not completely characterized) and found [58] to be luminescent, and the electrochemical oxidation and reduction of $Pt_2(POP)_4^{4-}$ have been carried out [59].

(i) Addition

Acetone and sulfur dioxide add to $Pt_2(POP)_4^{4-}$ with no change in the platinum oxidation state although both reactions lead to a loss of luminescence [27,57]. The addition of SO_2, which occurs reversibly in aqueous solution [57], is accompanied by a decrease in the intensity of the band at 368 nm and the appearance of a new band at 428.5 nm, assigned to the $^1A_{1g} \rightarrow {}^1A_{2u}$ transition of the parent compound shifted to lower energy by the addition of SO_2. The similarity of the ^{31}P NMR spectrum ($\delta = 65.01$; $^1J(PtP) = 3043$ Hz) to that of $Pt_2(POP)_4^{4-}$ and the magnitude of the PtP coupling constant (~ 3000 Hz) indicate the presence of a Pt(II)–Pt(II) dimer rather than a Pt(III)–Pt(III) one (for which $J(PtP) \sim 2000$ Hz) [60] during this reaction. Resonance Raman bands at 111, 220, 1112, and 1148 cm^{-1} are assigned to the Pt–Pt stretch, Pt–S stretch, and symmetric SO stretch for coordinated SO_2 and SO_2 dissolved in solution [61], respectively. The small difference between the Pt–Pt stretch in this adduct and that in the parent compound (116 cm^{-1} [38]) has been attributed to mass effects rather than to a change in the bonding. The atom attached to platinum has been identified as sulfur (on the basis of the 220 cm^{-1} band) and the attached species as sulfur dioxide rather than sulfite ion (from the higher energy of the SO symmetric stretch in this compound relative to that in $Rh_2(O_2CCH_3)_4$ species containing coordinated sulfite ion, 1000 and 933 cm^{-1} [62]). Since not all $Pt_2(POP)_4^{4-}$ was combined with SO_2 under the conditions of the experiment, the value of ϵ (4.1×10^4) for the adduct was calculated from its concentration as estimated from the equilibrium constant (1.74 mol^{-2} l^2) obtained from the spectral data.

An addition product was also reported [27] to result from the mixture of acetone with an aqueous solution of $Pt_2(POP)_4^{4-}$. The analysis of the resulting purple solid is consistent with the formula; $K_4Pt_2(POP)_4 \cdot 2H_2O \cdot (CH_3)_2CO$, but the nature of the interaction of the acetone with the platinum dimer is unclear since a crystal structure was not obtained and the formula also indicates the retention of two H_2O molecules (presumably in the apical positions). An interaction is clearly indicated, however, by the absence of luminescence in the solid state between 1.6 and 300 K, although luminescence is restored when the solid is dissolved in aqueous solution.

(ii) Reduction

The $Pt_2(POP)_4^{4-}$ species has been converted to a 5 − ion by pulse radiolysis [47] and to a 6 − ion by reduction with chromium(II) [57]. The $Pt_2(POP)_4^{6-}$ ion was characterized by the 1 : 2 $Pt_2(POP)_4^{4-}$: Cr(II) stoichiometry observed during a spectrophotometric titration with Cr(II),

which showed no evidence for a one-electron reduction product. The 6 − ion absorbs at 373 nm ($\epsilon = 9.6 \times 10^3$), 413 nm ($\epsilon = 1.0 \times 10^4$) and 459 nm ($\epsilon = 1.3 \times 10^4$) and its formation is accompanied by a decrease in the intensity of the band at 367 nm and the loss of emission at 514 nm. Resonance Raman yields a stretching frequency of 106 cm^{-1} (a decrease of 10 cm^{-1} from the value of 116 cm^{-1} observed for $Pt_2(POP)_4^{4-}$ itself), suggesting that the MO derived from the $6p_z$ orbital (populated upon reduction) is slightly antibonding.

The one-electron reduction product characterized during the pulse radiolysis of aqueous t-BuOH solutions [47] exhibits transient absorbances at 420 nm ($\epsilon = 1.3 \times 10^4$) and ca. 600 nm ($\epsilon = 1.7 \times 10^3$). The added electron is thought to enter a $p\sigma$ orbital ($^2A_{1g}$) rather a $d\sigma^*(d_{x^2-y^2})$ orbital and the absorbance at 420 nm is assigned to a $^2A_{1g} \rightarrow {}^2A_{2u}$ ($d\sigma^* \rightarrow p\sigma$) transition. The rate constant for the reaction of $Pt_2(POP)_4^{4-}$ with $e^-(aq)$ is 1.80×10^{10} M^{-1} s^{-1} while that for its disappearance (due to its re-oxidation) is 2.9×10^4 s^{-1}).

Reduction of $Pt_2(POP)_4^{4-}$ occurs at −0.43 V (H_2O, Ag/AgCl) in the presence of Mg^{2+} ion (differential pulse polarography) but cyclic voltammetric waves are seen only in the presence of halide ion [59] and only after at least one anodic sweep. Since the latter are attributed to the reduction of dihalo addition products, they will be discussed below. The lack of evidence for the production of the $Pt_2(POP)_4^{5-}$ ion alone is probably due to the rapid re-oxidation mentioned above.

(iii) Oxidation

In water, without added halide ion or in the presence of F^-, which is not complexed by the dimer, oxidation of $Pt_2(POP)_4^{4-}$ by differential pulse polarography yields $Pt_2(POP)_4(H_2O)_2^{2-}$ ($\lambda_{max} = 248$ nm [6,56]) at a peak potential of 0.69 V (glassy C, Ag/AgCl, pH = 6). When Cl^-, Br^-, or I^- ions are present however, the corresponding dihalo species are formed, at potentials of 0.56, 0.37 and −0.03 V, respectively. Spectral studies demonstrate the absence of substantial quantities of the mixed valence species, $Pt_2(POP)_4X^{4-}$, although the reduction is believed to proceed via this intermediate, which subsequently disproportionates [8]. Cyclic voltammetry (H_2O, glassy C) shows no waves without added halide ion and only irreversible ones in their presence ($E_{pa} - E_{pc} = 0.86$, 0.65, 0.25 V for Cl, Br, I). The oxidation potentials are dependent on the halide ion present ($E_{pa} = 0.53$, 0.35, −0.02 V for Cl^-, Br^-, I^-, respectively) but the reduction potentials are not ($E_{pc} = -0.33$, −0.30, −0.31 V for Cl^-, Br^-, I^-, respectively). This behavior is attributed to the formation of $Pt_2(POP)_4X^{5-}$ at the electrode prior to oxidation, with the halide ion providing a bridge for electron

transfer from the electrode to the platinum dimer, as suggested for the oxidation of Pt(II) monomers [63]. In CH_3CN, an anodic peak is observed at 0.78 V (vs. Ag/AgCl) which is independent of scan rate between 20 and 200 mV s^{-1}. At a scan rate of 1000 V s^{-1}, the anodic peak potential is 1.12 V and a small cathodic peak is seen at 0.61 V, from which $E^0 = 0.86$ V (midpoint of V_{ox} and V_{red}) for the one-electron oxidation of the parent compound.

(iv) Pt(III)–Pt(III) compounds

The first such species reported [10] were $Pt_2(POP)_4Cl_2^{4-}$ and $Pt_2(POP)_4(CH_3)I^{4-}$, formed by the oxidative addition of chlorine or iodomethane to $Pt_2(POP)_4^{4-}$. Di-adducts with Br [11,12], I [11], NO_2^- [13,15], SCN^- [6,15] and imidazolyl [15] are now known, as are mixed adducts, i.e. $Pt_2(POP)_4XY^{4-}$ (X = Cl, Br, I; Y = Cl, Br, I, CN, NO_2) [6,13,56]. These species have been synthesized by using oxidizing agents which also coordinate, separate oxidizing and coordinating agents, electrochemical oxidation, or substitution [13,56]. Their ease of formation and stability has been ascribed [4] to an increase in the bond order (from zero to one) due to the removal of two electrons from the $d\sigma^*$ orbital during oxidation. (Specific details for the preparation of individual compounds can be found in the appropriate references.)

Of the 15 compounds of the type $Pt_2(POP)_4XY^{4-}$ (X = Y = Cl, Br, I, NO_2, SCN, imidazolyl; X = Cl; Y = Br, NO_2; X = Br, Y = CN, NO_2; X = I, Y = Cl, Br, CH_3, NO_2, CN) prepared to date, 9 have been characterized structurally (X = Y = Cl [8,10], Br [11,12], I [11], NO_2 [13,14], SCN [14], imidazolyl [14]; X = I; Y = CH_3) [15]. These species all have the substituents in axial positions as represented schematically in Fig. 9, although specific bond distances may vary as seen in Table 1. (The dinitro adduct has been isolated both as a 4 − ion, as the potassium salt [14], and as an 8 − ion, as the sodium salt [13], with the latter having non-equivalent deprotonated pyrophosphites. In addition, the Pt–Pt bond length is significantly shorter in the sodium salt than it is in the potassium salt (2.733 Å vs. 2.754 Å).)

These compounds, which are diamagnetic, retain the 4 − charge of the parent ion (except for the sodium salt of the dinitro compound) and are reported [10] to be very stable in the solid as well as in solution (except for the CH_3I and NO_2 adducts [13]). The NMR spectra or derivatives with identical substituents are similar to those of the parent compound, consisting of a quintet of quintets for ^{195}Pt due to $^1J(PtP)$ and $^2J(PtP)$ and single resonances for ^{31}P, as expected for axial substituents, but become more complicated when the substituents differ (see Table 7 for δ and J values).

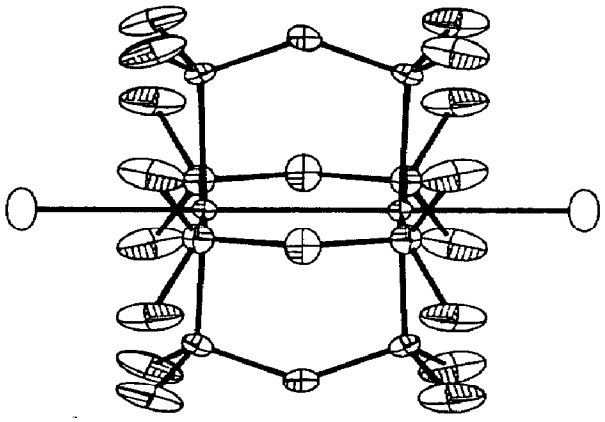

Fig. 9. Representation of structure of $Pt_2(POP)_4X_2^{4-}$. (Reprinted from ref. 12 with permission.)

The Pt–Pt distances in these species (Table 1) are at least 0.1 Å shorter than that in $Pt_2(POP)_4^{4-}$. They are also at least 0.1 Å longer than those in other Pt(III) dimers, which have been reviewed recently [64] and range from 2.461 in $Pt_2(SO_4)_4(H_2O)_2^{2-}$ [65] to 2.582 Å in $Pt_2(NH_3)_4(C_5H_4NO)_2^{2-}$ [9]. While the latter variations may be due to differences in bridging ligands, the former, where the $P_2O_5H_2^{2-}$ bridging groups are the same, should provide a valid measure of the bond strength. The Pt–Pt distances in $Pt_2(POP)_4XY^{4-}$, decrease in the order; $CH_3I > SCN > I > NO_2^* >$ imidazolyl* > Br > Cl. These results suggest that the Pt–Pt bond strength increases in the reverse order, i.e. $CH_3I < SCN < I < NO_2 <$ imidazolyl < Br < Cl, which agrees with that predicted on the basis of the σ *trans* effect [66], in which the Pt–Pt bond is weakened by the donation of electrons into the $d\sigma^*$ orbital. This same effect provides an explanation for the order of ν_{Pt-Pt} obtained [10] from resonance Raman spectra ($Cl^- > Br^- > I^-$) (Table 3) and for the energy of the $d\sigma \rightarrow d\sigma^*$ transition (discussed below).

The electronic spectra of these species show two bands (Table 2) [6,10], an intense high energy bond ($\lambda = 245$–345 nm, $\epsilon = 3$–5×10^4 cm^{-1} M^{-1}) and a less intense lower energy one ($\lambda > 335$ nm, $\epsilon > 8 \times 10^3$ cm^{-1} M^{-1}). This pattern has been reported previously [67] for species with a $(d\sigma)^2$ ground state, with the two bands being attributed to $d\sigma \rightarrow d\sigma^*$ and $d\sigma \rightarrow d\pi^*$ transitions. The energy of the $d\sigma \rightarrow d\sigma^*$ transition decreases in the order;

* Although two different Pt–Pt bond lengths have been found for the dinitro derivative, one of which is shorter than that for the imidazolyl adduct, this was obtained in the unusual deprotonated compound and the Pt–Pt distance from the more "normal" species is used in this comparison.

TABLE 7

NMR parameters for $Pt_2(POP)_4^{4-}$ and related species

Species	δ Pt (ppm)	^1J(PtP) (Hz)	^2J(PtP)	δ P (ppm)	^1J(PtP)	^2J(PtP)		Ref.
$Pt_2(POP)_4^{4-}$	−5139 [a]	3075		69.4 [a]				3
$Pt_2(PCP)_4^{4-}$	−5037	2490	7	97.0				77
$Pt_3(POPOP)_4^{6-}$	−4936	3250						58
	−4948	3300						
$Pt_2(POP)(SO_2)_2^{4-}$				65.01	3043			57
$Pt_2(POP)_4Cl_2^{4-}$	−4236 [b]	2175	88	27.96 [c]	2085			10
$Pt_2(POP)_4Br_2^{4-}$	−4544 [b]	2183	82	24.01	2100			10
$Pt_2(POP)_4I_2^{4-}$	−5103 [b]	2202	75	18.01	2148			10
$Pt_2(POP)_4CH_3I^{4-}$	−4311 [b]	2274	45.5	32.68	2274			10
	−5227 [b]	2454	85.7	30.32	2454			10
$Pt_2(POP)_4(NO_2)_2^{4-}$				30.9	2211			
$Pt_2(POP)_4(NO_2)Cl^{4-}$				32.9	2262	106	16.5	13
				26.7	2254	103		
$Pt_2(POP)_4(NO_2)Br^{4-}$				29.4	2258	104	16	13
				26.4	2264	101		
$Pt_2(POP)_4(NO_2)I^{4-}$				27.8	2290	93	16	13
				22.5	2232	101		
$Pt_2(POP)_4PhBr^{4-}$				37.0 [c]	2474			51
				32.6	2284			
$Pt_2(POP)_4(p\text{-}FC_6H_4)Br^{4-}$				36.2	2432			51
				31.9	2233			
$Pt_2(POP)_4PhI^{4-}$				31.6	2236			51
				30.5	2428			
$Pt_2(POP)_4(p\text{-}HOC_6H_4)Br^{4-}$				36.8	2468			51
				31.9	2233			
$Pt_2(POP)_4(p\text{-}MeOC_6H_4)Br^{4-}$				36.7	2441			51
				32.1	2222			
$Pt_2(POP)_4CNBr$	−4593	2224	102	26.08	2230			56
	−4101	1988	67	16.58	1993			
$Pt_2(POP)_4CNI$	−5087	2218	92	19.96	2219			56
	−4028	1934	57	15.40	2006			

[a] Relative to 1 M Na_2PtCl_6 external. [b] Relative to H_2PtCl_6 at 4218 MHz. [c] Relative to 85% H_3PO_4–15% D_2O external.

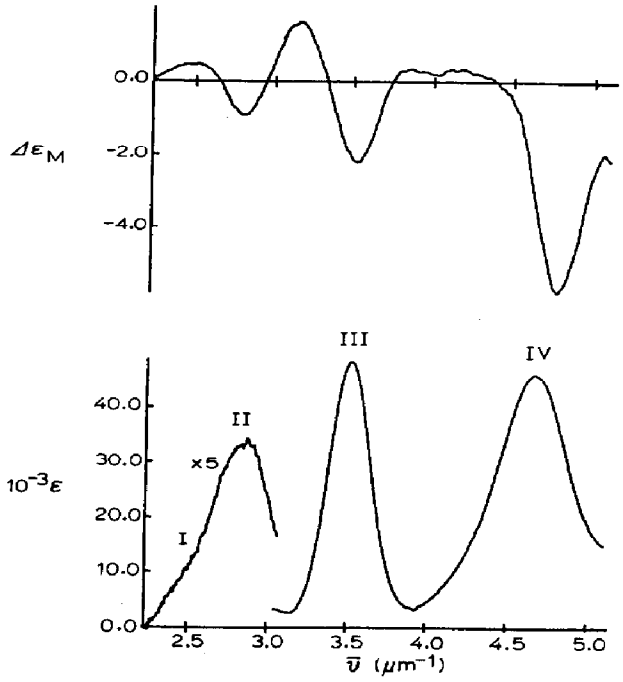

Fig. 10. Electronic absorption (lower curve) and MCD (upper curve) spectr $K_4Pt_2(POP)_4Cl_2$ in water. (Reprinted from ref. 24 with permission.)

$H_2O > Cl > Br >$ imidazolyl $> NO_2 > SCN > CH_3I > I$, in keeping wit *trans* effect which predicts a decrease in the energy of the $d\sigma^*$ orbital an increase in the σ donor ability of the ligand. The energy range obs for the $d\sigma \rightarrow d\sigma^*$ transition as the axial ligands are varied from H_2 SCN^- is much greater for Pt(III) than it is for Rh(II) (11000 vs. 7000 c [68], due to the greater degree of ligand character in the Pt–Pt bond.

The MCD spectra for $Pt_2(POP)_4X_2^{4-}$, X = Cl or Br, are very simil the absorption spectra of these species [24], as shown in Fig. 10. The an of these spectra is consistent with the assignments obtained previously analyses of the absorption spectra. (The original reference should be sulted for a further dissusion.)

Just as the apical ligands in $Pt_2(POP)_4XY^{4-}$ species exert a influence on the Pt–Pt bond, the Pt–Pt bond has an effect on the bonds (which can be evaluated from bond lengths and IR frequencies). Pt–X bond lengths in Table 1 are all greater than the corresponding v in monomeric platinum compounds (Table 8) and the Pt–X stret frequencies in the $Pt_2(POP)_4XY^{4-}$ species (Table 3) are lower than thc the respective monomers (Table 8). These results indicate that the I bond has a stronger *trans* influence than do the *trans* ligands in monomers, although it is weaker than that in other platinum(III) dime

TABLE 8

Pt–X distances and stretching frequencies in selected compounds

Compound	Pt–X(A)	ν_{Pt-X} (cm^{-1})	ν_{Pt-C} (cm^{-1})
K_2PtCl_4	2.316 [a]		
Cs_2PtCl_4	2.294 [b]	325, 330 [c]	
K_2PtCl_6	2.323 [d]	345, 344 [e]	
$(CH_3)_4NPtCl_6$	2.293 [f]		
Rb_2PtBr_4	2.435 [g]	208 [h]	
K_2PtBr_6	2.464 [i]	207 [j]	
Cs_2PtI_6	2.677 [k]	105.3 [j]	
$(PyH)_2PtI_6$	2.661 [l]		
trans-$PtCl(CH_3)[(PCH_3)_2]_2$		269–278 [m]	557–559 [m]
trans-$PtBr(CH_3)[PO(CH_3)_2]_2$			552 [m]
trans-$PtI(CH_3)[PO(CH_3)_2]_2$			546–551 [m]
trans-$Pt(CH_3)_4[PO(CH_3)_2]_2$			470 [m]
$(C_2H_5)N[Pt_2(H_2PO_4)_2(HPO_4)_2Cl_2]\cdot H_2O$	2.448 [n]		
$[Pt_2(NH_3)_4(C_5H_4NO)_2Cl_2](NO_3)_2$	2.444 [o]		
	2.429		
$[Pt_2(NH_3)_4(C_5H_4NO)_2Br_2](NO_3)_2$	2.573 [o]		
	2.562		
$[Pt_2(NH_3)_4(C_5H_4NO)_2(NO_2)_2](NO_3)_2$	2.172 [o]		
	2.168		

[a] R.H.B. Mais, P.G. Owstom, and A.M. Wood, Acta Crystallogr. Sect. B, 28 (1972) 393.
[b] E. Rodek, H. Bartl, W. Sterzel, and C. Platte, Neues Jahrb. Mineral. Monatsh., (1979) 81.
[c] P.L. Goggin and J. Mirk, J. Chem. Soc., Dalton Trans., (1974) 1479.
[d] R.J. Williams, D.R. Dillon, and W.D. Milligan, Acta Crystallogr., Sect. B, 29 (1973) 1369.
[e] P. Labonville, J.R. Ferraro, S.M.C. Wall, and L.J. Basile, Coord. Chem. Rev., 7 (1972) 257.
[f] R.W. Berg and I. Sotofte, Acta Chem. Scand. Sect. A, 32 (1978) 241.
[g] E. Rodek, W. Stertzel, H. Bartl, and W. Schuckmann, Neues Jarhb. Mineral, Monatsh., (1979) 277.
[h] Y.M. Bosworth and R.J.H. Clark, J. Chem. Soc., Dalton Trans., (1974) 1749.
[i] H.D. Grundy and I.D. Brown, Can. J. Chem., 48 (1970) 1151.
[j] (a) G. Thiele, C. Mrozek, K. Wittman, and H. Wirkner, Naturwissenschaften, 65 (1978) 206. (b) G.C. Messner, E.L. Amma, and J.A. Ibers, Inorg. Chem., 6 (1967) 725. (c) R. Eisenberg and J.A. Ibers, Inorg. Chem., 4 (1965) 773.
[k] G. Thiele, C. Mrozek, D. Kammerer, and K. Wittman, Z. Naturforsch., Teil, B 38 (1983) 905.
[l] G. Thiele and D. Wagner, Z. Anorg. Allg. Chem., 446 (1978) 126.
[m] (a) J.D. Ruddick and B.L. Shaw, J. Chem. Soc. A., (1969) 2801. (b) J.D. Ruddick and B.L. Shaw, J. Chem. Soc. A, (1969) 2964.
[n] D.P. Bancroft, F.A. Cotton, L.R. Falvello, S. Han, and W. Schwotzer, Inorg. Chim. Acta, 87 (1984) 147, and references therein.
[o] L.S. Hollis, M.M. Roberts, and S.J. Lippard, Inorg. Chem., 22 (1983) 3637.

Many of the di-adducts undergo displacement reactions with other substituents. For example, $Pt_2(POP)_4X_2^{4-}$ (X = Cl, Br, I, NO_2) will react with Y^- (Y = Cl, Br, I) to form $Pt_2(POP)_4Y_2^{4-}$ (although Cl^- will not replace

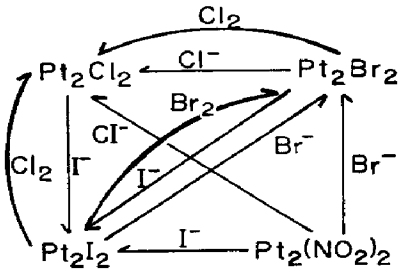

Fig. 11. Reaction scheme showing interconversion of $Pt_2(POP)_4X_2^{4-}$ species. (Pt_2 represents $Pt_2(POP)_4$.)

coordinated I^-) [13,56]. The dihalides also react with halogens according to the usual activity series, i.e., Cl_2 will replace Br^- or I^- and Br_2 will replace I^-, as summarized in Fig. 11. The intermediate $Pt_2(POP)_4(NO_2)Y^{4-}$ (Y = Cl, Br) has been detected in the displacement of NO_2 by these two halide ions [13] and mixed halide intermediates have been seen when small amounts of halogen are used. (Although similar intermediates have not been reported in the thermal exchange of halide ions, they may be present and have been found when these reactions are activated photochemically, vide infra.) The halide exchange is thought to occur by the loss of ions whereas NO_2 rather than NO_2^- is lost in the dinitro case. Mixed adducts can also be formed by the reaction of $Pt_2(POP)_4^{4-}$ with a small quantity of halogen, Y_2, in the presence of halide ion X^- (X = Cl, Y = Br, I; X = Br, Y = I), in analogy with Pt(IV) chemistry [69] or with interhalogens. In the latter case, an excess of the interhalogen, XY, will result in the formation of $Pt_2(POP)_4X_2^{4-}$ as the major product (X is the more electronegative group in XY).

These halide substitutions can be enhanced photochemically, in some cases by several orders of magnitude. (The replacement of I^- by Cl^- is complete in a few minutes, while there is no thermal reaction over a period of days.) They proceed via mixed halide intermediates and occur with quantum yields greater than unity. It has been suggested that the mechanism involves the loss of a halogen atom to generate the mixed valence species, $Pt_2(POP)_4X^{4-}$, via an $X \rightarrow Pt(III)$ LMCT excited state, in analogy with the reactions of Pt(IV) complexes which are also enhanced by light and proceed with $\phi > 1$ [70].

Studies of the equation of $Pt_2(POP)_4Cl_2^{4-}$ yield a value of 9×10^{-6} s^{-1} for the formation of the aquo-chloro species [71]. This is slightly faster than the rate of equation calculated for the $PtCl_6^{2-}$ ion (5×10^{-7} s^{-1}), but several orders of magnitude slower than that for $Pt_2(\mu\text{-}PO_4H)Cl_2^{4-}$, in which the first and second chloride ions are replaced with rate constants of 8 and 5×10^{-2} s^{-1}, respectively. The origin of this large difference in reactivity is unclear at the present time.

The ions $Pt_2(POP)_4^{4-}$ and $Pt_2(POP)_4Cl_2^{4-}$ have been found [56] to behave as dibasic acids with $pK_1 = 3.10$ and 4.95 and $pK_2 = 6.75$ and 7.55, respectively. The monodeprotonated complexes are stable in aqueous solution, but the doubly-deprotonated species deposit metallic platinum rapidly. The state of protonation has also been found to affect the rate of substitution, with Cl^- replacing either Br^- or I^- and Br^- and I^- displacing one another in the X_2 complexes at pH = 6.5 but not at pH < 4, although substituted deprotonated complexes have not been observed.

The dihalo derivatives have been reduced electrochemically [59] in aqueous solution ($E = -0.18$, -0.21, -0.11 V for Cl^-, Br^-, I^-, respectively), a process which is thought to occur through the disproportionation of the mixed valence intermediate, $Pt_2(POP)_4X^{4-}$, discussed in the next section.

(v) Pt(II)–Pt(III) species

A number of mixed-valence materials including $Pt_2(POP)_4^{3-}$ and $Pt_2(POP)_4X^{3-}$ (X = Cl, Br, I) have been characterized. The former has been cited as a product in photoionization [72] and pulse radiolysis [73] studies of the $Pt_2(POP)_4^{4-}$ ion while the latter are formed by the partial oxidation of the parent (II/II) compound in the presence of halides [8,12,39].

The irradiation of $Pt_2(POP)_4^{4-}$ ions in water at 355 nm [72] yields $Pt_2(POP)_4^{3-}$ and hydrated electrons, identified from the appearance and behavior of transient absorption spectra, which show an increase in absorbance at 320 and 720 nm and a decrease at 368 nm (relative to the parent compound). The presence of hydrated electrons is inferred from the wavelength of the 720 nm band and its kinetic behavior toward O_2 and $H_2PO_4^-$ [74]. The remainder of the transient, which resembles the spectrum obtained during the pulse radiolysis of the bisimidazole adduct of $Pt_2(POP)_4^{4-}$ and that observed when the parent compound is irradiated in the presence of electron acceptors [4], is attributed to the $Pt_2(POP)_4^{4-}$ excited state. The products are believed to be formed by a two-photon process, with the second photon liberating the electron from the triplet excited state (produced by the first photon). This scheme is supported by the dependence of the production rate on laser power, which is sigmoidal as the power is varied from 1 to 12 mJ per pulse.

The reaction of hydroxyl radicals, generated by pulse radiolysis, with $Pt_2(POP)_4^{4-}$ has also been reported [73] to yield $Pt_2(POP)_4^{3-}$, ($\lambda_{max} = 310$ nm, $\epsilon = 7.6 \times 10^4$ M^{-1} cm^{-1}). The rate of appearance of this band is first order in each reactant with a second-order rate constant of 8×10^9 M^{-1} s^{-1}. It subsequently decays by a second-order path ($k = 6.7 \times 10^8$ M^{-1} s^{-1}) to produce a band of lower intensity at 368 nm (characteristic of the original dimer) and one at 248 nm (attributed to $Pt_2(POP)_4^{2-}$). The 310 nm band of

the mixed-valence species also appears during the laser excitation (355 nm) of $Pt_2(POP)_4^{4-}$ solutions as a decay product of the excited state (demonstrated by its bands at 330 and 470 nm). (When the irradiation is carried out at pH 6, a broad band at 700 nm due to hydrated electrons is also seen.)

The $Pt_2(POP)_4X^{4-}$ species have been synthesized by adding a limited amount of the appropriate halogen along with the halide ion to an aqueous solution of the (II/II) species [8,12,39] or by combining equimolar amounts of the (II/II) and (III/III) species in aqueous solution. The golden metallic products have been shown by X-ray crystallography to contain infinite Pt–Pt–X–Pt–Pt–X chains. Single crystals of the bromo compound exhibit semiconductor behavior with an electrical conductivity between 5×10^{-4} and 10^{-3} Ω^{-1} cm^{-1}). Even a pressed powdered sample of the iodo compound (for which single crystals could not be grown) gave a value of 2.8×10^{-6} Ω^{-1} cm^{-1} [8], which is many times greater than the conductivity found for other mixed-valence platinum species such as $[M(II)L_4][M(IV)L_4X_2][ClO_4]$ which range from 10^{-12} to 10^{-8} Ω^{-1} cm^{-1} [75].

The Pt–Pt distances in these mixed-valence species (2.813 and 2.793 Å for X = Cl and Br, respectively) are intermediate between those in the parent compound (2.925 Å) and the corresponding dioxidized materials (Pt–Pt = 2.695 and 2.723 Å for Cl_2 and Br_2, respectively). The bromide atom is equidistant between the platinum atoms of adjacent dimers (Pt–Br = 2.699 Å) [8], but two different Pt–Cl distances are found (2.367 and 2.966 Å) [12]. These results suggest that the chloride is best described as a localized-valence, Pt(II)/Pt(III), species whereas the bromide (studied crystallographically) and the iodide, which has been examined spectroscopically [39], are more delocalized. A similar situation is found for these same halides in Wolfram's red-type salts, which contain Pt(II) and Pt(IV) ions in localized (chloride) and delocalized (bromide and iodide) environments [75]. The electronic spectra of these solids exhibit intense bands at 512, 645, and 870 nm (Cl, Br, and I, respectively) which have been attributed to inter-valence transitions, by analogy with those seen in the spectra of a number of "platinum blues" [76]. Three other metal-based bands are also present in the spectra of these compounds (Table 2).

Resonance Raman spectra [39] for the inter-valence bands of these mono-halo species show fundamentals at 291, 210, and 185 cm^{-1} for the chloro, bromo, and iodo species, respectively. The chloro compound exhibits a lengthy progression of overtones for this vibration, while the bromo-species shows a shorter one and the iodo- species, no overtones at all, indicating a decreasing degree of asymmetry with increasing atomic weight. The rR values for ν_{PtPt} occur at 152 (Cl), 117 and 122 (Br), and 100 (I) cm^{-1}, all of which are less than those found for ν_{PtPt} in the corresponding dihalo species (Table 3). These results can be attributed to the bridging behavior of the

halogens in the mono-halo species. (The chloro species also shows excitation profiles for both ν_{PtPt} and ν_{PtCl} which increase substantially on the low energy side of the intervalence band by analogy with Wolfram's red-type salts.) Finally, these mixed-valence species display a weak, very broad ESR signal which increases slightly in intensity as the temperature is lowered from 295 to 120 K and in the order Cl < Br < I, which offers further support to the view of increased delocalization with increasing atomic weight suggested by X-ray and Raman results.

(vi) Other derivatives

Two other related species have been synthesized to date, a higher oligomer studied only in solution [58], and a species with methylenebis(phosphinic acid) bridges characterized structurally as well as spectroscopically [77].

The former compound was obtained as a dark green powder by heating K_2PtCl_4 and H_3PO_3 to 170 °C rather than 100 °C. It is soluble only in water where it decomposes within a few hours (first to the dimeric species and finally to the monomer). The initial blue solutions exhibit an intense band at 580 nm ($\epsilon = 5.0 \times 10^4$ M^{-1} cm^{-1}) with weaker bands at 360 nm ($\epsilon = 2.5 \times 10^3$ M^{-1} cm^{-1}) and 260 nm ($\epsilon = 7.0 \times 10^3$ M^{-1} cm^{-1}). Excitation of aqueous 1 M HCl solutions at 360 and 580 nm produces an intense red luminescence ($\tau < 0.5$ μs) at 650 nm. The large red shift (from 368 nm to 580 nm) seen for the absorbance of the Pt–Pt bond or going from the dimer to the higher oligomer has also been observed for rhodium isocyanide complexes in solution [18,78,79]. Magnetic susceptibility and EPR measurements show the platinum atoms to be diamagnetic, as expected for platinum(II), while NMR spectra are consistent with the oligomeric structure proposed. Specifically, the ^{195}Pt NMR spectrum exhibits two poorly resolved quintets of unequal intensity centered at $\delta = -4936$ (J(Pt–P) = 3250 Hz) and $\delta = -4948$ (J(Pt–P) = 3300 Hz) (relative to H_2PtCl_6 at 42.8 MHz) while the ^{31}P NMR shows a broad overlapping multiplet centered at $\delta = 62.1$ with satellite peaks due to coupling with Pt-195 (J(Pt–P) = 3250 Hz). The broadness of the line ($\nu_{1/2} = 112$ Hz) is due to second order coupling as well as to nonequivalent phosphorus nuclei. Vibrational spectra for this species show a Raman band at 85 cm^{-1} and an infrared band at 147 cm^{-1}. The similarity of these values to the two Pt–Pt stretching modes predicted on the basis of a linear trimeric platinum model, a Raman-active mode at 82 cm^{-1} and an IR-active mode at 142 cm^{-1}, offer additional support for the characterization of this species as a trimer.

The methylenebis(phosphinic acid) bridged species, $K_4Pt_2(PCP)_4$ (PCP = $P_2CH_4O_4^{2-}$), can be prepared by heating a solution of K_2PtCl_4 and K_2PCP at pH 5 to 100 °C for 72 h [77]. This species has four-fold

symmetry, with a slightly longer Pt–Pt bond than that in the parent compound (2.980 Å vs. 2.925 Å), although the other bond lengths are similar (Table 1). The absorbance behavior of this compound and that of $K_4Pt_2(POP)_4$ are very similar at 77 K (Table 2), although λ_{max} for the $Pt_2(PCP)_4^{4-}$ ion is slightly higher than that for the $Pt_2(POP)_4^{4-}$ ion. When the emission behavior at 295 K is compared, however, it can be seen that while λ_{em} is very similar for the two compounds, the lifetimes and quantum yields are much smaller for the methylene-bridged species, due primarily to the higher nonradiative rate constant. Indeed, the lifetimes at 77 K are the same (10 μs), due to a decrease in temperature. Converting the CH_2 groups of the ligands to CD_2 groups produces a small (10%) increase in the lifetime. The species undergoes oxidative addition with halogens to give the corresponding $Pt_2(PCP)_4X_2^{4-}$ ions. The substitution of CH_2 for O decreases the acidity of the species; pK_1 and $pK_2 = 8.0$ and 11.0, respectively, vs. 3.0 and 8.0, respectively, which may be related to the observation that the new compound is more stable to hydrolysis at high pH values than is the original one.

G. CONCLUSION

The discussion above has been an attempt to summarize the behavior of the $Pt_2(POP)_4^{4-}$ ion which has emerged during the ten years that it has been known. The novel aspects of the behavior of this and related species and the pace at which investigations into this behavior has been proceeding make it likely that the past ten years represent only the beginning of a long period of study for this compound. It is hoped that this review may help to further such studies.

ACKNOWLEDGEMENT

The author thanks Carol Creutz of Brookhaven National Laboratory for originally suggesting the subject of this review and providing the surroundings in which work on it was begun.

REFERENCES

1 R.P. Sperline, M.K. Dickson, and D.M. Roundhill, J. Chem. Soc. Chem. Commun., (1977) 62.
2 A.D. Troitskaya, Russ. J. Inorg. Chem., 6 (1961) 585.
3 M.A. Filomena Dos Remedios Pinto, P.J. Sadler, S. Neidle, M.R. Sanderson, A. Subbiah, and R. Kuroda, J. Chem. Soc., Chem. Commun., (1980) 13.
4 C.-M. Che, L.G. Butler, and H.B. Gray, J. Am. Chem. Soc., 103 (1981) 7796.
5 K.A. Alexander, S.A. Bryan, M.K. Dickson, D. Hedden, and D.M. Roundhill, Inorg. Synth., 26 (1986) 211.

6 C.-M. Che, L.G. Butler, P.J. Grunthaner, and H.B. Gray, Inorg. Chem., 24 (1985) 4662.
7 R.E. Marsh and F.H. Herbstein, Acta Crystallogr., Sect. B 39 (1983) 280).
8 C.-M. Che, F.H. Herbstein, W.P. Schaefer, R.F. Marsh, and H.B. Gray, J. Am. Chem. Soc., 105 (1983) 4604
9 L.S. Hollis, M.M. Roberts, and S.J. Lippard, Inorg. Chem., 22 (1983) 3637.
10 C.-M. Che, W.P. Schaefer, H.B. Gray, M.K. Dickson, P.B. Stein, and D.M. Roundhill, J. Am. Chem. Soc., 104 (1982) 4253.
11 K.A. Alexander, S.A. Bryan, F.R. Fronczek, W.C. Fultz, A.L. Rheingold, D.M. Roundhill, P. Stein, and S.F. Watkins, Inorg. Chem., 24 (1985) 2803.
12 R.J.H. Clark, M. Kurmoo, H.M. Dawes, and M.B. Hursthouse, Inorg. Chem., 25 (1986) 409.
13 D. Hedden, D.M. Roundhill, and M.D. Walkinshaw, Inorg. Chem., 24 (1985) 3146.
14 C.-M. Che, W.-M. Lee, T.C.W. Mak, and H.B. Gray, J. Am. Chem. Soc., 108 (1986) 4446.
15 C.-M. Che, T.C.W. Mak, and H.B. Gray, Inorg. Chem., 23 (1984) 4386.
16 W.A. Fordyce, J.G. Brummer, and G.A. Crosby, J. Am. Chem. Soc., 103 (1981) 7061.
17 (a) K.W. Hipps, G.A. Merrell, and G.A. Crosby, J. Phys. Chem., 80 (1976) 2232.
(b) K.W. Hipps, G.A. Merrell, and G.A. Crosby, J. Phys. Chem., 82 (1978) 1454.
18 K.R. Mann, J.G. Gordon, and H.B. Gray, J. Am. Chem. Soc., 97 (1975) 3553.
19 S.F. Rice and H.B. Gray, J. Am. Chem. Soc., 105 (1983) 4571.
20 W.L. Parker and G.A. Crosby, Chem. Phys. Lett., 105 (1984) 544.
21 F. Perrin, Ann. Phys., 12 (1929) 169.
22 Y. Shimizu, Y. Tanaka, and T. Azumi, J. Phys. Chem., 88 (1984) 2423.
23 W.A. Fordyce, and G.A. Crosby, J. Am. Chem. Soc., 104 (1982) 985.
24 H. Isci and W.R. Mason, Inorg. Chem., 24 (1985) 1761.
25 J.M. Solar, M.A. Ozkan, H. Isci, and W.R. Mason, Inorg. Chem., 23 (1984) 758.
26 W.B. Heuer, M.D. Totten, G.S. Rodman, E.J. Hebert, H.J. Tracy, and J.K. Nagle, J. Am. Chem. Soc., 106 (1984) 1163.
27 J.T. Markert, D.P. Clements, M.R. Corson, and J.K. Nagle, Chem. Phys. Lett., 97 (1983) 175.
28 J.N. Demas, and G.A. Crosby, J. Am. Chem. Soc., 93 (1971), 2841, in K. Kalyanasundaram, Coord. Chem. Rev., 46 (1982) 159.
29 Y. Shimizu, Y. Tanaka, and T. Azumi, J. Phys. Chem., 89 (1985) 1372.
30 J.S. Griffith, The Theory of Transition Metal Ions, Cambridge University Press, London, 1964, p. 113.
31 D.S. Martin Jr., M.A. Tucker, and A.J. Kassman, Inorg. Chem., 4 (1965) 1682.
32 (a) W.A. Fordyce, and G.A. Crosby, Inorg. Chem., 21 (1982) 1455.
(b) W.A. Fordyce, H. Rau, M.L. Stone, and G.A. Crosby, Chem. Phys. Lett., 77 (1981) 405.
33 W.A. Fordyce and G.A. Crosby, J. Am. Chem. Soc., 104 (1982) 985.
34 Y. Tanaka and T. Azumi, Inorg. Chem., 25 (1986) 247.
35 J.B. Birks, Photophysics of Aromatic Molecules, Wiley-Interscience, New York, 1970.
36 G.F. Steinmakh, and M.P. Tsvirko, Opt. Spectrosc., 49 (1980) 278.
37 M.K. Dickson, S.K. Pettee, and D.M. Roundhill, Anal. Chem., 53 (1981) 2159.
38 P. Stein, M.K. Dickson, and D.M. Roundhill, J. Am. Chem. Soc., 105 (1983) 3489.
39 M. Kurmoo and R.H.J. Clark, Inorg. Chem., 24 (1985) 4420.
40 C.J. Ballhausen, Molecular Electronic Structures of Transition Metal Complexes, McGraw Hill, London, 1979, pp. 132–135.
41 C.-M. Che, L.G. Butler, H.B. Gray, R.M. Crooks, and W.H. Woodruff, J. Am. Chem. Soc., 105 (1983) 5492.

42 S.F. Rice and H.B. Gray, J. Am. Chem. Soc., 103 (1981), 1593.
43 J. Gulen and J.A. Page, J. Electroanal. Chem., 67 (1976) 215.
44 L. Meites, P. Zuman, W.J. Scott, B.H. Campbell, and A.M. Kartos, Electrochemical Data, Part I, Wiley, New York, 1974, AG85.
45 G. Navon and N. Sutin, Inorg. Chem., 13 (1974) 2159.
46 A. Vogler and H. Kunkely, Angew. Chem., Int. Ed. Engl., 23 (1984) 316.
47 C.-M. Che, S.J. Atherton, L.G. Butler, and H.B. Gray, J. Am. Chem. Soc., 106 (1984) 5143.
48 C.R. Bock, J.A. Connor, A.R. Gutierrez, T.J. Meyer, D.G. Whitten, B.P. Sullivan, and J.K. Nagle, J. Am. Chem. Soc., 101 (1979) 4815.
49 J.R. Peterson and K. Kalyanasundaram, J. Phys. Chem., 89 (1985) 2486.
50 (a) M.Z. Hoffman, D.R. Prasd, G. Jones, and V. Malba, J. Am. Chem. Soc., 105 (1983) 6360.
(b) H.P. Sullivan, W.J. Dressick, and T.J. Meyer, J. Phys. Chem., 86 (1982) 1473.
51 D.M. Roundhill, J. Am. Chem. Soc., 107 (1985) 4354.
52 C.-M. Che and W.-M. Lee, J. Chem. Soc. Chem. Commun. (1986) 512.
53 D.M. Roundhill and S.J. Atherton, Inorg. Chem., 25 (1986) 4071.
54 (a) J. Kochi, Organometallic Mechanism and Catalysis, Academic Press, New York, 1978, Chap. 7.
(b) R.A. Rossi and R.H. deRossi, Aromatic Substitutions by the $S_{RN}1$ Mechanism, ACS Monograph 178, American Chemical Society, Washington, DC, 1983.
55 G.W. Parshall, J. Am. Chem. Soc., 96 (1974) 2360.
56 S.A. Bryan, M.K. Dickson, and D.M. Roundhill, J. Am. Chem. Soc., 106 (1984) 1882.
57 K.A. Alexander, P. Stein, D.B. Hedden, and D.M. Roundhill, Polyhedron, 2 (1983) 1389.
58 M.K. Dickson, W.A. Fordyce, D.M. Appel, K. Alexander, P. Stein, and D.M. Roundhill, Inorg. Chem., 21 (1982) 3857.
59 S.A. Bryan, R.H. Schmehl, and D.M. Roundhill, J. Am. Chem. Soc., 106 (1986) 5408.
60 M.K. Dickson, Ph.D. Thesis, Washington State University, 1982.
61 E.R. Lippincott and F.E. Walsh, Spectrochim. Acta, 17 (1961) 123.
62 I.B. Baranovskii, S.S. Abdullaev, G.Ya. Mazo, and R.N. Schchelokov, Russ. J. Inorg. Chem., 27 (1982) 305.
63 R.F. Lane and A.T. Hubbard, J. Phys. Chem., 81 (1977) 734, and references therein.
64 F.A. Cotton and R.A. Walton, Struct. Bonding (Berlin), 62 (1985) 1.
65 (a) G.S. Muraveiskaya, G.A. Kukina, V.S. Orlova, O.N. Evstafeva, and M.A. Porai-Koshits, Dokl. Akad. Nauk SSSR, 226 (1976) 76.
(b) D.P. Bancroft, F.A. Cotton, L.R. Falvello, S. Han, and W. Schwotzer, Inorg. Chim. Acta, 87 (1984) 147.
66 C.H. Langford and H.B. Gray, Ligand Substitution Processes, Benjamin, Menlo Park, CA, 1965, p. 27.
67 N.S. Lewis, K.R. Mann, J.G. Gordon II, and H.B. Gray, J. Am. Chem. Soc., 98 (1976) 7461.
68 V.M. Miskowski, T.P. Smith, T.M. Loehr, and H.B. Gray, J. Am. Chem. Soc., 107 (1985) 7925.
69 A. Peloso, Coord. Chem. Rev., 10 (1973) 123.
70 (a) R.L. Rich and H. Taube, J. Am. Chem. Soc., 76 (1954) 2608.
(b) A.W. Adamson and A.H. Sporer, J. Am. Chem. Soc., 80 (1958) 3865.
71 R. El-Mehdawi, S.A. Bryan, and D.M. Roundhill, J. Am. Chem. Soc., 107 (1985) 6282.
72 K.C. Cho and C.M. Che, Chem. Phys. Lett., 124 (1986) 313.
73 D.M. Roundhill and S.J. Atherton, J. Am. Chem. Soc., 108 (1986) 6829.

74 (a) M.S. Matheson, in R.F. Gould (Ed.), Solvated Electron, Adv. Chem. Ser., 50 (1965) 46.
(b) M. Anbar and P. Netra, Int. J. Appl. Radiat. Isot., 18 (1967) 493.
75 R.J.H. Clark, Adv. Infrared Raman Spectrosc., 11 (1984) 95.
76 (a) L.S. Hollis and S.J. Lippard, J. Am. Chem. Soc., 103 (1981) 1330.
(b) L.S. Hollis and S.J. Lippard, J. Am. Chem. Soc., 103 (1981) 6761.
77 C. King, R.A. Auerbach, F.R. Fronczek, and D.M. Roundhill, J. Am. Chem. Soc., 108 (1986) 5626.
78 I.S. Sigal and H.B. Gray, J. Am. Chem. Soc., 103 (1981) 2220.
79 K.R. Mann, N.S. Lewis, R.M. Williams, H.B. Gray, and J.G.H. Gordon, Inorg. Chem., 17 (1978) 828.